This document contains:

1. Detailed response to referees' comments and suggestions
2. List of minor updates in data analysis
3. List of minor updates in data presentation

1. Detailed response to referees' comments and suggestions

Referee #1 (Remarks to the Author):

In general, the paper is thoughtful, well-written, and a welcome addition to the literature.The dataset(s) presented are well-validated by the authors (to the extent possible), andcould be very useful for other Earth System studies. I congratulate the authors for thisnice contribution.

> We thank the referee for reviewing our work and for the positive evaluation of the study. Please find our point-by-point response below.

My primary criticism of the paper is the choice to use the JPL RL05 data rather thanthe RL06 data (released in October 2018), primarily due to timeliness. Understand-ably, much of the analysis was likely done prior to the release of the RL06 data, and itwould require substantial efforts to redo the analysis. The authors did show that the re-constructions were much more sensitive to the choice of precipitation dataset than theGRACE data, so it is entirely plausible that calibrating the model to RL06 data wouldmake little difference in the results. The hesitation comes with an anticipated use-caseof the dataset, as mentioned by the authors (abstract and introduction), which is to fillthe gap in between GRACE and GRACE-FO and to "reconcile" the two datasets. Thefirst GRACE-FO data will be in so-called "RL06" data standards. It would behoove theauthors to address this discrepancy, and provide some analysis/insights on whetherany conclusions change when using RL06 data to calibrate the model. The authorsdiscuss the potential for errors in low degree spherical harmonics (Section 4.3), and infact, many of the changes from RL05 to RL06 occur in the low degree harmonic coef-ficients for the JPL data product, including the "mean pole correction" of the C21/S21coefficient as recommended by Wahr et al., 2015.

> Thank you very much for this suggestion. In our revised version of the manuscript, we use RL06 instead of RL05. While this did not massively improve or change the reconstructions, it ensures future consistency with the first GRACE-FO data from JPL.

Specific Comments:

Section 2.3.2: The model is calibrated independently for each mascon. It is unclearto me – does this mean for the JPL data product it is done on each 3-degree mas-con,

while on the GSFC data product it is done on each 1-degree mascon? Thereare many more mascons in the GSFC data product than degrees of freedom in the GRACE dataset – but perhaps this does not matter for the model calibration sincespatial correlations are taken into account. Can you comment?

Yes, as mentioned in section 2.3.1, the calibration is conducted at each mascon (3° for JPL and 1° for GSFC). Because GRACE effective resolution is lower than 1°, neighboring GSFC mascons essentially represent the same signal as you mentioned. However, this does not really matter for the model calibration and we found no indication that calibrating the model at GSFC resolution (1°) leads to overfitting or unreasonable parameter values. In fact, the MCMC algorithm does not provide only one model parameter set at a given mascon, but a (more robust) distribution of acceptable model parameter sets. These parameter distributions do exhibit spatial auto-correlation, reflecting the spatial "smoothness" or oversampling inherent to the GSFC solution.

Figure 4c and 4d: It is unclear to me what each data point represents. Is each dot fora single mascon?

Yes, this has been made clearer in the legend of Figure 4.

Section 3.4: The title "Global Average" is perhaps misleading since it does not includeocean areas. Suggested revision.

Title changed to "Global land averages"

Figure 7: Are these simply the global average (area weighted) of Figure 5 and 6?

Thank you very much for this question. No, Figure 7 depicts box and whisker plots of the values shown in Figure 5 and 6 (we follow the general convention of 10^{th}, 25^{th}, 50^{th}, 75^{th}, and 90^{th} percentiles). Note that the calculation of the percentiles takes into account mascon area (coastal JPL mascons that have a smaller area have a smaller weight). This has now been made clearer in the legend of Figure 7, as well as of Figures 10, 12 and 13 which have similar representations.

Section 4.3: This analysis is done excluding Greenland and Antarctica. Are Greenland nd Antarctica excluded from the actual GRACE data (JPL and GSFC) when computing correlations/RMS with altimetry/steric information in Figure 11b/c? I wonder what the impact of including/excluding it is? Presumably small, but some discussion on this would make for a better comparison.

Yes, Greenland and Antarctica are excluded for all products, mainly because WRR models are not meant to be used in those regions and thus either do not provide output or produce spurious values in those regions. We checked this and found that including Greenland and Antarctica only has a small effect. The agreement with altimetry-steric decreases for some

WRR models and for JPL mascons and slightly increases for GSFC mascons and some of the reconstructions. Because this additional analysis (including Greenland and Antarctica) does not provide a fair basis for comparing all the different products (because of the WRR models), we prefer to exclude it. We note that global means both excluding or including Greenland and Antarctica are also readily available as part of the final product.

Section 4.3: It is hypothesized that low degree errors could be responsible for theGRACE data having a worse correlation than the modeled data. I agree. I could alsoenvision errors in high degrees also being a culprit. The mascon solutions used intheory do not necessitate any post-processing, but it is very likely that residual longi-tudinal stripes remain. The GRACE-REC model should not calibrate to these resid-ual stripes, but rather the signal since the stripes are more stochastic in nature frommonth to month. However, it is plausible that residual stripes could contaminate corre-lation/RMSE comparison with a detrended/deseasoned timeseries of presumed oceanmass from sea level budget analysis (altimetry/steric).

Thank you for this comment, we were not aware of this possibility. This has been included in the discussion: *"... (e.g. caused by errors in low degree spherical harmonics or residual longitudinal stripes)..."*.

Section 4.4: Could you include some discussion of the length of the timeseries of theBSWB data? Figure 12 is confusing because in Figure 12a, the BSWB data does notoverlap with the GRACE data record. However, Figure 12b/c compare the BSWB datawith the actual GRACE data – inherently implying some overlap.

Thank you for this remark. The BSWB data in theory covers the period 1979-2015, however, calculation of the basin-scale water balance is also subject to availability of runoff measurements which varies a lot depending on the basin. Thus, while BSWB data shown in Figure 12a is not available after 1998, many stations do overlap with the GRACE period. Our intention for selecting the Ob basin in Figure 12a was also to illustrate how the reconstruction can reconcile gaps between datasets from multiple sources.

This has been made clearer in the text: *"The temporal coverage of BSWB estimates at each river basin thus depends on the availability of runoff data and does not always cover the GRACE time period."*

Section 4.4 and 4.5: In both sections it is pointed out there is slightly better performance in GSFC than JPL, and this is potentially owed to the better spatial resolution of theGSFC data. Did you apply the scale factors to the JPL data? These are designedto reduce such leakage error on the basin scale. If not, I suggest doing so for thisanalysis. Second, when making these comparisons, is the length of the data record always consistent? The JPL data both begins before, and extends after, the GSFCdata. The tails of the GRACE dataset are of worse quality, and I am curious if the inclusion of these extra months on the JPL data is perhaps responsible for the inferior performance.

Thank you for this comment. We note that this point is only valid for section 4.4 as GRACE data is not used in section 4.5. It is true that the CLM4-based scale factors could be applied to JPL data when recovering the basin averages used for the analysis in section 4.4. We now apply the scale factors for this analysis (now noted in the figure legend). Also we made sure that both JPL and GSFC are evaluated over the same time period.

We also rephrased the sentence to make clear that our intention here is to explain why GSFC-based products seem to have better performance than the JPL-based products in sections 4.4. and 4.5. We have added the following clarification: *"This mainly occurs because the meteorological forcing is aggregated at a resolution of 1° in the case of GSFC-based products, allowing the GSFC reconstructions to provide a slightly more localized signal."*

Referee #2 (Remarks to the Author):

In their study the authors use three different precipitation and temperature products toreconstruct past variability of terrestrial water storage (TWS) from 2017 back to 1901.The reconstruction is performed by estimating the parameters of a statistical modelwhich is calibrated by relating precipitation and temperature to observed TWS from theGRACE satellite mission. To account for temporally and spatially correlated errors inthe reconstructed TWS the authors apply a spatial autoregressive model to generatea large number of ensemble members representing the uncertainty of the estimatedTWS anomalies. Afterwards, the derived reconstructions are evaluated against differ-ent independent datasets, showing the value of the dataset for different hydrological and climate applications.

The presented data and method are new and sufficiently described in the text. Longand consistent time series of TWS as presented here will be very useful in future formany different user groups, thus it is a valuable contribution to ESSD.

Generally, the manuscript is well structured and well written. Data access is easy andwell documented. Downloaded data are ready to use without problems. The data is ofhigh quality as shown by the authors in several appropriate evaluations.

We thank the referee for reviewing our work and for the positive evaluation of the study. Please find our point-by-point response below.

General comments:

Chapter 2.2: Instead of ERA-Interim as used in the study, it would be better to usethe new ERA5 reanalysis (at least for the next update of the reconstruction, as ERA-Interim production will eventually end). Probably this would even improve the quality ofthe reconstruction.

Thank you for this suggestion. In our revised version of the manuscript, we use the newly available ERA5 instead of ERA-Interim. We confirm that the quality of the ERA5-driven reconstruction improved very much as a result of this change. ERA-Interim-based products often had the lowest performance among all reconstructions, but as a result of the update, ERA5-based reconstructions now often yield the best performance. Figure legends and in-text discussions have been updated where necessary.

Chapter 2.3: Some aspects of the modelling approach are unclear to me: Where does Eq. 5 come from? A sentence on this for explanation would be helpful forthe reader.

Thank you for this comment. We realize that this was not entirely clear. We have a made a minor adjustment to Equation 1, which now leads Equation 5 to be more intuitive. In practice, this modification does not change the reconstructed signals. The full development of how Equation 5 is obtained is also provided and illustrated in the Supplementary Material.

Equation 5 is also better explained in the main text: "*The initial value of the storage is thus obtained as the ratio between the rate of water input and the rate of water loss (also see the full development in Supplementary Information)*"

Does time t in Eq. 6 refer to months and TWS(t) to a monthly average (in contrast tobefore, where t was time in days)? If so, the notation should be adjusted accordingly,e.g. using t' and mean(TWS) to distinguish monthly from daily resolution.εalso de-pends on (monthly) t, this should be indicated in Eq. 6 (and accordingly in Eq. 8), e.g.withε_t'.

Thank you for noting this. We have replaced t with t_m whenever we referred to monthly resolution. Equations in the remainder of the manuscript have been updated accordingly.

Chapter 2.4.2:I do not understand Eq. 13: To my understanding σ_η is the "variance of the autoregressive process" (line 8) which should be "larger than that of the driving white noise process" (line 9), which is σ_ε. However, for large autocorrelation φ the expression √(1-φˆ2) approaches zero, thus σ_η is smaller than σ_ε for any autocorrelation differ-ent from zero. Please comment on this.

Thank you for your question. There was apparently some confusion, σ_η is the variance of the noise process and σ_ε is the variance of the auto-regressive process, not the other way around. Taking this into account, your interpretation of the equation is entirely correct. This was made clearer in the text: "*This accounts for the fact that the variance of an autoregressive process ($\boldsymbol{\sigma_\varepsilon}$) is larger than that of the driving white noise process ($\boldsymbol{\sigma_\eta}$).*"

Specific comments:

P. 5, line 9: (typo) adjustement must be adjustment

Corrected, thank you.

P. 9, line 20: (Eq. 8) dependence on time for GRACEREC andεshould be visible inequation.

Corrected, thank you.

P. 12, line 9: does “ensemble hindcast” refer to a mean of all 6 reconstructions (eachwith 100 ensemble members)? Please point this out more clearly. Otherwise, pleaseindicate which reconstruction is evaluated.

Thanks for this comment. This evaluation is for the 100 ensemble members of the JPL-MSWEP reconstruction. This is now indicated in the caption.

P. 13, line 19: so no SAR model was used for daily products? Maybe mention this andthe reason for it explicitly.

Thank you for noting this. Yes, the reason is that calibrating a robust SAR model for the daily resolution is impossible since GRACE observations are at monthly resolution. This was added to the main text: “*The reason for this is that no SAR model (Section 2.4.2) can be reliably calibrated at the daily resolution as the two training GRACE datasets have monthly resolution*”

P. 15, line 13ff: Did you evaluate the difference between the two GRACE solutions in advance? Usually, GRACE solutions of different processing centers do not differlargely, thus it is not surprising that they lead to similar reconstructions.

We agree that this is not too surprising, however, because we get this question a lot, this is why we conducted this assessment.

P. 16, line 19ff: This is a repetition of P. 14, line 10-13. It should be summarized anddiscussed at one location.

Thank you, this was corrected.

P. 17, line 5: The GRACE solution from Graz is officially called ITSG-Grace2018 (notjust ITSG2018). Mayer-Gürr et al., 2016 is an outdated reference; if you used the2018 solution, please cite: Mayer-Gürr, Torsten; Behzadpur, Saniya; Ellmer, Matthias;Kvas, Andreas; Klinger, Beate; Strasser, Sebastian; Zehentner, Norbert (2018): ITSG-Grace2018 - Monthly, Daily and Static Gravity Field Solutions from GRACE. GFZ DataServices. http://doi.org/10.5880/ICGEM.2018.003

Thank you, we have updated the reference and figure legends accordingly.

P. 19, line 8f: Please comment on how this is possible since GRACE cannot resolvefeatures as small as 1◦.

We agree that the wording was inadequate. We have replaced "the higher spatial *resolution* of the GSFC mascons" with "the higher spatial *sampling* of the GSFC mascons".

We also rephrased the sentence to make clear that our intention here is to explain why GSFC-based products seem to have better performance than the JPL-based products in sections 4.4. and 4.5. We have added the following explanation: "*This mainly occurs because the meteorological forcing is aggregated at a resolution of 1° in the case of GSFC-based products, allowing the reconstruction to provide a slightly more localized signal.*"

P. 19, line 19: "size smaller than..." Do you mean "size larger than..."? Otherwise Ido not understand why you only use the very small basins.

Thank you for noting this. Here, we focus on basins that are small enough to completely fall within the footprint of a GRACE mascon or a WRR2 grid cell. The main reason for this is that the number of large basins available prior to 1980 is extremely small compared to the thousands of measurements made at small basins back until 1901 and before. We are aware that large-scale mass changes are not necessarily representing the dynamics of such small catchments. However, the purpose is not to obtain a perfect match, but to diagnose potential relative changes over time in the performance of the century-long reconstruction. We have added the following explanation in the main text:

"*The reason for focusing on small basins is that a much larger number of them is available in the early century (compared to the number of large basins, which are the focus of section 4.4). We note that the unavoidable mismatch between large-scale mass changes and local catchment runoff dynamics is to some extent alleviated by the spatial coherence of anomalies in weather patterns at yearly scale.*"

P. 19, line 20: "leaving 12'496 stations", please indicate number of stations for each time period, as in Figure 13c only 9306 stations are evaluated.

Thank you for noting this. This is now indicated in the legend: *"(n=1274, 8065 and 9306 for 1901-40, 1941-80 and 1981-2010 respectively).*"

Figure 1b: y-axis label should be changed from cm H2O to TWS [cm]

Corrected.

Figure 3 caption, line 2: delete "also"

Corrected.

Figure 4: a, b and e are too small. In c, only one x-axis label is printed, please addmore.

Corrected.

Figure 7: Please mention to what the bars and lines refer to. Standard deviation, minand max? Is the global mean computed with or without Greenland and Antarctica?

Thank you for this feedback, we agree that the legend needed more clarity. Figure 7 depicts box and whisker plots of the values shown in Figure 5 and 6 (we follow the general convention of 10^{th}, 25^{th}, 50^{th}, 75^{th}, and 90^{th} percentiles). Note that the calculation of the percentiles takes into account mascon area (as coastal JPL mascons can have a smaller area). This has been made clearer in the legend of Figure 7, as well as of Figures 10, 12 and 13 which have similar representations. Greenland and Antarctica are always excluded from these figures.

Figure 8: In 8a for some time series (red, purple, light blue) the numbers at the scaleare missing. b and c are too small to distinguish different reconstructions.

The missing numbers were added in 8a. With respect to 8b and 8c, the fact that the different reconstructions are difficult to distinguish in terms of inter-annual variability (over the GRACE time period) is actually the correct interpretation of this figure. We have made this clearer in the text and note that the different reconstructions can also be better distinguished in 8a.

Figure 13d: Repetition of legend from 13b would be nice, to see at a glance what isdisplayed here.

Corrected, thank you.

Referee #3 (Remarks to the Author):

General Comments: The paper "GRACE-GEC: a reconstruction of climate-driven water storage changes ofthe last century" presents a set of statistical models of TWS trained to two GRACEmascon solutions using multiple precipitation and temperature forcing inputs. The dis-cussion in the paper well framed, providing a detailed methodology and explanationof relevant key decisions in developing that methodology. The paper then provides aproduct description and evaluation that conveys the information content of the devel-oped models and provides an analysis of that content in a straightforward and logicalway. The paper itself is well written, and I

did not find any typographical errors or major grammatical issues anywhere. The level of detail is such that anyone generally familiarwith the subject matter can nicely comprehend the discussed work and outcomes. Asa whole, I believe that this paper is very close to a final form, and primarily have clari-fication questions and small probing questions that I would like to possibly see furtherdiscussed.

> We thank the referee for reviewing our work and for the positive evaluation of the study. Please find our point-by-point response below.

Data access was straightforward and is well documented. My only suggestion would beto have a more meaningful naming schema for the zip files. For example, a name thattells me "trained with JPL, forced by MSWEP, spanning 1979-2016", as in the namesof the NetCDFs themselves, rather than requiring that I refer to the README for thatinformation.

> Thanks for this comment. We have made the .zip file names more meaningful.

As for ease of use, I was able to create a Jupyter Notebook with Python3.7 in under two minutes that already had me using the data. The choice of NetCDF isvery much appreciated.

As a general comment, with the release of JPL's RL06 Mascons, do you plan to updatethe JPL-trained models? Or perhaps more generally, is there a plan in place to con-tinually produce new models when new GRACE solutions are available for training?

> In response to a suggestion by another referee, we have updated the JPL dataset used here to RL06. As discussed in section 4.1.1, we find that the reconstructions are not very sensitive to the employed GRACE training dataset. We would update the model if 1) there is a major breakthrough in GRACE processing technique or 2) we find a significantly improved and still as simple formulation of TWS changes (i.e. Eq. 1).

Similarly, when GRACE-FO is operational, what plan is in place to extend the trainingdatasets with new months? Will this be continually re-done, or is there even a benefit todoing a new run with each new month?

> With the exception of the two cases mentioned just above, the plan is to update the ERA-5 version on a yearly basis (or occasionally more frequently upon reasonable request), provided the corresponding author is able to secure both funding and time for making these updates.

A general comment in the paper discussing thesensitivity of the models to additional months of GRACE forcing would be appreciated.

Thanks for this comment. This has been added in the main text: *"[…] updates of the two reconstructions driven by ERA5 will be published when needed. We note that because including additional GRACE months only barely improves the quality of the model fit, no systematic re-calibration of the models is planned at this stage."*

Specific Comments:

- p. 5 line 5 / Table 1 - Did you consider using formulations of the two mascon solutionsthat have equivalent GIA models removed? For example, on looking at the GSFCmascon website, those mascons are distributed with either the A et al. model or ICE-6G model removed. You could compute consistent reconstructions for both masconsets but using consistent GIA models. Also, does any of this matter since you are usinga detrended dataset for the training of your reconstructions? This should probably be clarified.

Thanks for this comment. Yes, it actually does not really matter since the detrended dataset is used during model training. This has been clarified in section 2.3.2: *"We note that as a result, the choice of the GIA model used in GRACE processing (Table 1) does not impact the model calibration"*

- p. 5 line 5 / Table 1 - For JPL, why have you selected the CRI filtered solutionand what considerations must be made as a result of that choice? Are you usingthat solution at it's gridded resolution (0.5 degree x 0.5 degree) or on a mascon-by-mascon basis (4551 mascons). If at the gridded level, are you forcing reconstructionoutputs to be equal over all grid cells in each mascons or allowing for spatial variationwithin individual mascons? Same question for the temperature and precip inputs overthese mascons? Also, are there any other differences between the mascons that areimportant to consider (or alternatively, is this even in the scope of your paper)?

Thank you for this comment. The CRI filtered solutions are recommended by JPL for land hydrology analyses. The meteorological forcings are averaged over the footprint of the land part of the mascons. This has been made clearer in the text of section 2.3.1: "*The meteorological forcing is always spatially averaged over the spatial footprint of the GRACE mascons*.".

Training is always done at mascon-scale (mascon-by-mascon basis) as mentioned in section 2.3.1. Concerning the differences in terms of the processing of these solutions, they certainly exist and the methodologies are well described by the cited references. We do not extensively discuss these differences here as 1) this would be outside the scope of the paper, and 2) the choice of the training GRACE dataset was found to be of secondary importance (as shown in section 4.1.1), so that, even if we would include such a discussion, it would not really aid the interpretation of our results.

- Section 2.1 - Relating to the last two questions, do you handle each solution at

theirown native resolutions or are they placed onto a common grid? It appears that themodel outputs from the GSFC-driven runs were placed onto a half-degree grid. Howwere they handled in the training portion of the products developments?

Thanks for this comment. As mentioned above and in section 2.3.1, all model training and model output is handled at the mascon level. Final products are provided on a half-degree grid as this seems to be the most convenient for most users.

- p. 8 line 9 - Why is the seasonal cycle removed prior to the calibration step? What arethe repercussions of this decision on the reconstruction? This is somewhat addressedin Section 3 but at the time is a major open question to the reader.

Thank you for this comment. Removing the seasonal cycle allows us to focus the model on those deviations from typical TWS variability that are hard to predict (while seasonality is easily defined from GRACE data alone). This is now better explained in section 2.3.2: "*Removing the seasonal cycle lets the model calibration focus on capturing the inter-annual variability correctly*".

This has little repercussion on the reconstruction, except that the reconstruction likely cannot be used investigate long-term changes in seasonality as mentioned in section 3.1.

- p. 8 line 20 - In your discussion of error sources, how do spatially correlated errors inthe GRACE solutions impact the work? You have "mascon binned" your reconstruction,so to speak, but the GRACE mascons themselves are not independent mass estimates(especially in the case of the 1-arc-degree GSFC mascons). This bias error source isin addition to the measurement errors from GRACE and is difficult to address. Haveyou included anything to account for this?

Thanks for this comment. This is true, we implicitly include this type of errors in the SAR model. This is now more clearly mentioned in section 2.4.1: *"They include measurement and leakage errors from GRACE"*.

As mentioned by the referee, spatially correlated errors in GRACE arise for a variety of reasons, and are difficult to address and to isolate. In our case, the SAR model can only provide a bulk representation of the spatial-temporal structure and magnitude of these errors. Our intention is to provide an overall estimate of the expected mismatch between the reconstruction and GRACE data (a mismatch caused by a wide variety of factors, including the interdependence of neighboring mascons). Our goal with the ensemble members is that this error estimate will also be easily computed when the end user wants to perform spatial and/or temporal aggregation.

- p. 16 line 18-22 - This seems redundant with section 3.5.

Thank you, this has been corrected.

- p. 16 line 23-p. 17 line 2 - It is unclear if/why this is unexpected. If training was doneat the mascons scale, it would seem that larger scales aggregating multiple masconswould show well calibrated agreement se a necessary but not sufficient condition on the dataset.

We were not entirely sure how to interpret/understand this comment. We mean that calibrating the relationships locally does not automatically ensure that the global averages will also match. For instance, having poor model skill over several key regions (see e.g. Figures 5 and 6) could have contaminated the global averages, but this is not the case here.

- Section 4.2 - In addition to the lower spatial resolution, the Kalman smoothed dailyGRACE solution is correlated in time; is your comparison to the GRACE-REC productsat all different than for the monthly solutions as a result of this?

Thank you for this comment. The actual (true) TWS itself can be expected to be highly auto-correlated, especially at the daily scale, however, it is also true that the Kalman smoothing could further increase the autocorrelation of the time series. This is now mentioned in the text: *"(note that the solution is also correlated in time as a result of the Kalman smoothing)"*.

While additional smoothing likely negatively affects all skill scores shown in Fig.10bc, we do not think that this would bias the comparison between WRR2 and GRACE-REC products (none of the two should be more affected than the other by this issue).

- Figure 7 - The dark/light distinction could be a little more obvious, rather than havingto read deeply into the caption, and also have a stronger contrast.

We have made the distinction more obvious by enhancing the contrast and have added a legend in the figure.

- p. 19 line 8 - GSFC mascons are smaller, yes, but does the GSFC solution actuallyhave better resolution than the JPL mascons? This is related to the comments abouthow the JPL mascons are handled and how spatial correlations in the solutions arehandled (ex: higher cross-mascon correlations in the GSFC solution than with JPL dueto the smaller mascon sizes).

Thank you for this comment. Our understanding is that both solutions have approximately the same effective spatial resolution. What we mean here is that, because the meteorological forcing is aggregated over a smaller footprint in the case of GSFC, the GSFC reconstructions occasionally provide a more localized estimate of TWS changes. We do not mean to say that GRACE GSFC has higher resolution than GRACE JPL.

This has been made clearer in the text, also in response to a previous comment from another referee: *"This mainly occurs because the meteorological forcing is aggregated at*

a resolution of 1° in the case of GSFC-based products, allowing the reconstruction to provide a slightly more localized signal."

- In the abstract, possible user groups and applications were identified. Would anexample of the application of this work in one of those areas be within the scope of thispaper? Also, if the reconstruction is based on de-seasoned and de-trended GRACEinformation, is bridging the GRACE/GRACE-FO gap actually an application? Whatlimitations are placed on such a use?

Thank you for these questions. One use case is already implicitly illustrated with the sea level budget in section 4.3. In fact, over 1993-2002, Figure 11a provides a reconstruction-based estimate of the inter-annual variability in the steric contribution. Benchmarking of global hydrological models is also implicitly included in Figures 7, 9, 10, 11, 12 and 13. The first publication describing this type of approach (Humphrey et al. 2017) provides an example application relating to estimating groundwater depletion and Figure 1 in Humphrey et al. 2018 also contains an example of inter-disciplinary application.

As for bridging GRACE/GRACE-FO, we agree that this paper only potentially resolves the question of the inter-annual variability. This should be seen as preparatory work. Our opinion is that the seasonal cycle estimated from GRACE could be in theory extended to cover the data gap without major issues from a climatological point of view (if GRACE and GRACE/FO happened to largely diverge in terms of seasonality, this would rather indicate a problem with the geodesy). With respect to the trends, we anticipate that they could be relatively safely extrapolated for the duration of the data gap, however, this would require a more thorough assessment. We would be very interested to follow-up on this particular application as soon as the first GRACE-FO data becomes available.

2. List of updates in data analysis

1. JPL RL05 was replaced with JPL RL06
2. ERA-Interim was replaced with ERA5, leading to a significant improvement.
3. Equations (1) and (5) were slightly modified. In practice, this has no impact on the reconstructed signals.
4. For consistency, all models were re-trained and all products were updated in the online data repository. This new version (v3) replaces the previous version (v3beta).

3. List of changes in data presentation

1. The development leading to Equation (5) is now explained in a Supplementary Information.
2. For completeness and in response to a user request, we also illustrate the 2003-2014 GRACE trends, reconstructed GRACE-REC trends and WRR2 trends in Supplementary Figures S2-S4.

GRACE-REC: a reconstruction of climate-driven water storage changes over the last century

Vincent Humphrey[1,2], Lukas Gudmundsson[1]

[1] Institute for Atmospheric and Climate Science, ETH Zurich, Switzerland
[2] Division of Geological and Planetary Sciences, California Institute of Technology, Pasadena, CA, USA

Correspondence to: Vincent Humphrey (vincent.humphrey@env.ethz.ch)

Abstract.

The amount of water stored on continents is an important constraint for water mass and energy exchanges in the Earth system and exhibits large inter-annual variability at both local and continental scales. From 2002 to 2017, the satellites of the Gravity Recovery and Climate Experiment mission (GRACE) have observed changes in terrestrial water storage (TWS) with an unprecedented level of accuracy. In this paper, we use a statistical model trained with GRACE observations to reconstruct past climate-driven changes in TWS from historical and near real time meteorological datasets at daily and monthly scales. Unlike most hydrological models which represent water reservoirs individually (e.g. snow, soil moisture, etc.) and usually provide a single model run, the presented approach directly reconstructs total TWS changes and includes hundreds of ensemble members which can be used to quantify predictive uncertainty. We compare these data-driven TWS estimates with other independent evaluation datasets such as the sea level budget, large-scale water balance from atmospheric reanalysis and in-situ streamflow measurements. We find that the presented approach performs overall as well or better than a set of state-of-the-art global hydrological models (Water Resources Reanalysis version 2). We provide reconstructed TWS anomalies at a spatial resolution of 0.5°, at both daily and monthly scales over the period 1901 to present, based on two different GRACE products and three different meteorological forcing datasets, resulting in 6 reconstructed TWS datasets of 100 ensemble members each. Possible user groups and applications include hydrological modelling and model benchmarking, sea level budget studies, assessments of long-term changes in the frequency of droughts, the analysis of climate signals in geodetic time series and the interpretation of the data gap between the GRACE and the GRACE Follow-On

mission. The presented dataset is publicly available (https://doi.org/10.6084/m9.figshare.7670849) and updates will be published regularly.

Contents

Supprimé: 9

Supprimé: 9

Supprimé: 14

Supprimé: 15

Supprimé: 17

Supprimé: 20

Supprimé: 21

1 Introduction

Because the amount of freshwater available on land controls the development of natural ecosystems as much as human activities, terrestrial water storage (TWS) represents a critical variable of the Earth system. Changes in TWS can be caused by both anthropogenic and natural processes. Natural variability in ocean and atmospheric circulation, such as the El Niño Southern Oscillation (ENSO), is responsible for anomalies in precipitation which strongly influence water storage (Ni et al., 2017), leading to regional droughts and floods with large impacts on human activities (Veldkamp et al., 2015). At the global scale, climate-driven fluctuations in the total amount of water stored on land have been linked to a wide range of geophysical phenomena, including changes in global mean sea level (Cazenave et al., 2014;Reager et al., 2016;Rietbroek et al., 2016;Dieng et al., 2017), changes in global carbon uptake by land ecosystems (Humphrey et al., 2018), and the motion of the Earth's rotational axis (Adhikari and Ivins, 2016;Youm et al., 2017). In addition to climate-driven natural variability, human activities also influence terrestrial water storage, for instance through groundwater depletion (Rodell et al., 2009;Chen et al., 2016), building of dams (Chao et al., 2008), or the impact of anthropogenic climate change on land ice (Jacob et al., 2012).

From 2002 to 2017, changes in terrestrial water storage (TWS) have been measured by the GRACE satellites with an unprecedented accuracy. Because these observations integrate both natural and anthropogenic effects across all water reservoirs (i.e. soil moisture, groundwater, snow, lakes, wetlands, rivers and land ice), isolating the contribution of specific reservoirs or the relative importance of natural versus anthropogenic effects is still relatively uncertain and has been the focus of several recent publications (Reager et al., 2016;Eicker et al., 2016;Wada et al., 2016;Fasullo et al., 2016;Felfelani et al.,

2017;Getirana et al., 2017;Pan et al., 2017;Andrew et al., 2017;Rodell et al., 2018;Hanasaki et al., 2018;Khaki et al., 2018;Cazenave, 2018). In this context, one critical aspect is to model the effect of climate variability on TWS changes. At this time, only global hydrological models and land surface models can provide long-term estimates of natural TWS variability, however, they are usually not calibrated against GRACE measurements and sometimes exhibit large biases in TWS amplitude (Schellekens et al., 2017;Zhang et al., 2017;Scanlon et al., 2018). Typically, only a small number of such model runs is available and exploring the uncertainty related to the use of different meteorological forcing datasets is not possible. With this paper, we aim to address these shortcomings with a computationally cheap alternative. Unlike hydrological models which represent physical processes and model water reservoirs individually (e.g. snow, soil moisture, lakes, etc.), we train a statistical model to directly reconstruct the total TWS changes from precipitation and temperature information.

The primary objective of this paper is to provide long and consistent time series of climate-driven TWS variability. Although the temporal coverage of GRACE observations will be extended by the GRACE Follow-On mission launched on May 22 2018, there will be a temporal gap of approximately one year between the two missions. The reconstruction provided here is calibrated against GRACE measurements and can be used to interpret this data gap and reconcile the two datasets. In addition, we provide a century-long TWS reconstruction that can be used to study past natural TWS variability. We expect that this product will be relevant to sea level budget studies (Chambers et al., 2016;Cheng et al., 2017;Frederikse et al., 2018;Cazenave, 2018), the analysis of climate signals in geodetic time series (in GRACE or in e.g. ground GNSS measurements), development of daily hydrological loading models (Dill and Dobslaw, 2013;Moreira et al., 2016), as well as global to regional assessments of the recurrence of extreme hydrological droughts and their impact on ecosystems (Sheffield and Wood, 2007;Sheffield et al., 2012;Beguería et al., 2014;Griffin and Anchukaitis, 2014;Kusche et al., 2016;Dai and Zhao, 2016;Spinoni et al., 2017;Heim, 2017;Rudd et al., 2017;Sinha et al., 2017;Haslinger and Blöschl, 2017;Um et al., 2017;Bento et al., 2018;D'Orangeville et al., 2018;Huang et al., 2018;Markonis et al., 2018;Anderegg et al., 2018;Gao et al., 2018).

2 Data and Methods

2.1 GRACE products

The two different monthly GRACE solutions used here (Table 1) are obtained using the so-called mass concentration (mascon) technique. This technique provides estimates of mass changes over small predefined regions, that are referred to as *mascons*. The two solutions differ in terms of the employed processing algorithms and also in terms of the models used to correct for the effect of glacial isostatic adjustment (GIA). For more general information on the GRACE mission, gravity recovery techniques and processing, we refer the reader to the reviews of Wouters et al. (2014) or Wahr (2015).

2.2 Precipitation and temperature

We use three different precipitation products which are aimed to address the needs of various user communities (Table 2). The multi-source weighted-ensemble precipitation dataset (MSWEP) merges a large number of existing precipitation products, including satellite-based, raingauge-based and reanalysis products (Beck et al., 2017;Beck et al., 2018). We expect this dataset to provide a best-estimate for the period 1979-2016. The Global Soil Wetness Project Phase 3 (GSWP3) forcing dataset (Kim, 2017) is based on the 20th Century Reanalysis (20CR) version 2c (Compo et al., 2011). The original 20CR precipitation fields produced at a resolution of 2° are dynamically downscaled using spectral nudging and bias-corrected using observations from the Global Precipitation Climatology Project (GPCP) and the Climatic Research Unit (CRU). With this dataset, we aim to provide a homogeneous long-term reconstruction of climate-driven TWS changes over the period 1901-2014. Third, we use precipitation estimates from the European Centre for Medium-Range Weather Forecast (ECMWF) re-analysis (ERA5), which cover the period 1979-present. With this dataset, we aim to provide frequent updates of reconstructed TWS anomalies which can, for instance, be used to investigate the data gap between the GRACE mission (decommissioned in October 2017) and the GRACE Follow-On mission launched in May 2018. For temperature, we use ERA5 air temperature in combination with MSWEP and ERA5 precipitation, and GSWP3 air temperature in combination with GSWP3 precipitation. We note that sensitivity analyses have shown that the choice of the temperature dataset has very little influence on the final product (not shown).

Supprimé: e

Supprimé: -Interim

Supprimé: -Interim

Supprimé: -Interim

2.3 Modelling approach

2.3.1 Model formulation

A simple statistical model is calibrated at each GRACE mascon individually, meaning that model parameters are space-dependent. One model is calibrated for each combination of the two GRACE products (Table 1) with the three precipitation products (Table 2). The meteorological forcing is always spatially averaged over the spatial footprint of the GRACE mascons. Because the model described here does not have any explicit constraint in terms of mass or energy conservation, we refer to it as a statistical model, however its formulation is largely inspired from basic principles of hydrological modelling. Assuming a linear water store model, water outputs are directly proportional to the storage and to the residence time of the water store (e.g. Beven, 2012), so that the temporal evolution of the storage can be approximated as:

$$\mathrm{TWS(t)} = \big(\mathrm{TWS(t-1)}\big) \cdot \mathrm{e}^{-\frac{1}{\tau(t)}} + \mathrm{P(t)} \qquad (1)$$

where t is a daily time vector, $TWS(t)$ is the storage, $P(t)$ is the precipitation input and $\tau(t)$ is the residence time of the water store.

Small (large) values of the residence time indicate that water inputs tend to leave the reservoir quickly (slowly), either through runoff or evapotranspiration. Here we introduce seasonal changes in residence time (e.g. related to snow accumulation during the cold season or increased evaporative demand during the warm season) using a temperature-dependent relationship. The residence time used in Eq. (1) is formulated as a function of de-trended daily air temperature:

$$\tau(t) = a + b \cdot T_Z(t) \qquad (2)$$

Supprimé:

Supprimé: +P(t)

Where a and b are calibrated model parameters with positive sign and $T_Z(t)$ is a transformation of the original de-trended daily air temperature $T(t)$. The purpose of this transformation is to first make τ only sensitive to changes in temperature when temperature is higher than 0° Celsius,

$$T_0 = \begin{cases} 0, & T < 0 \\ T, & T \geq 0 \end{cases} \quad (3)$$

and to moderate the influence of extreme temperature values by applying a sigmoid transform to the standardized temperature:

$$T_Z = 1 - \tanh\left(\frac{T_0 - \mathrm{Mean}(T_0)}{\mathrm{StDev}(T_0)}\right) \quad (4)$$

As a result of this transformation, T_Z approaches a value of 1 (0) when temperature gets colder (warmer) and thus the residence time increases (decreases) (Eq. 2). Note that different or more complex formulations (e.g. also involving net radiation) were tested but did not yield significant improvement compared to the relatively simple approach presented here. The result of this model is illustrated in Fig. 1a, which depicts the temperature-dependent residence time (red line), the daily precipitation input (blue bars) and the resulting terrestrial water storage time series (blue line).

The initial value of the storage ($TWS(t)$ at $t = 0$) is computed from the analytical solution for the equilibrium state of Eq. (1) given the mean precipitation input and the mean residence time:

$$\mathrm{TWS}(0) = \frac{\mathrm{Mean}(P)}{1 - \mathrm{Mean}\left(e^{-\frac{1}{\tau(t)}}\right)} \quad (5)$$

The initial value of the storage is thus obtained as the ratio between the mean rate of water input and the mean rate of water loss (also see the full development in Supplementary Information). Using this solution (Eq. 5) requires the assumption that the storage is close to equilibrium at the start of the reconstruction but avoids the loss of six years for model spin-up as was done in previous work (Humphrey et al., 2017).

Supprimé: .

Supprimé: a

Supprimé: $\bar{P}$

Supprimé: $\bar{P} \cdot -\log\left(\mathrm{mean}\left(e^{-\frac{1}{\tau(t)}}\right)\right)^{-1}$

Still, we note that reconstructed TWS anomalies at the very beginning of the time series (typically the first year) should be interpreted with care.

2.3.2 Model calibration

The daily water storage time series (Eq. 1) is averaged to monthly temporal resolution (t_m) in order to make it comparable with the monthly GRACE time series. Calibration is conducted at monthly scale against de-seasonalized and de-trended GRACE TWS observations (Fig 1b), such that:

$$\mathrm{anom}\big(GRACE(t_m)\big) = \beta \cdot \mathrm{anom}\big(TWS(t_m)\big) + \varepsilon \qquad (6)$$

where β is a calibrated scaling factor, ε corresponds to an error term and $\mathrm{anom}()$ is an operator indicating that the seasonal cycle and the linear trend are removed as mentioned above. The trends are removed during model calibration because many trends in GRACE are caused by anthropogenic activities (Humphrey, 2017;Rodell et al., 2018), which our climate-driven model cannot explain by definition. We note that as a result, the choice of the GIA model used in GRACE processing (Table 1) does not impact the model calibration. Removing the seasonal cycle lets the model focus on capturing the inter-annual variability correctly. The three model parameters (a, b: Eq. 2 and β: Eq. 6) are calibrated at each mascon using a Markov Chain Monte Carlo (MCMC) procedure minimizing the sum of squares of the residuals between the predicted and observed monthly TWS anomalies (Haario et al., 2006;Humphrey et al., 2017). The MCMC procedure provides distributions of equally acceptable parameter sets which are later used in the generation of ensemble members (section 2.4).

2.4 Generation of ensemble members at monthly resolution

2.4.1 Rationale for the generation of model ensembles

The empirical residuals (ε) in Eq. (6) correspond to the difference between observed and predicted water storage anomalies. They include measurement and leakage errors from GRACE, structural model errors and errors introduced by the imperfect meteorological forcing. In this section, we aim to quantify and

Supprimé: t_m

Supprimé: t_m

communicate the magnitude of these errors to end users in a practical way. A classical approach is to provide the standard error σ_ε for every mascon $m_{1,\dots,i,\dots,n}$ (Fig. 2a):

$$\sigma_\varepsilon(m_i) = \sqrt{\text{Variance}[\varepsilon(m_i)]} \quad (7)$$

Because it can be shown in our case that the residuals are normally distributed (Fig. 2b), it is relatively safe to use the standard error to estimate the predictive uncertainty (and any confidence interval) over a given mascon. However, in many applications, predictions from individual mascons need to be aggregated, for instance to compute basin-scale averages or global means. In this case, obtaining an error estimate for the aggregated value is not trivial because the spatial covariance of the errors needs to be taken into account during the error propagation (Bevington and Robinson, 2003). Because errors are spatially and temporally correlated, any averaging operation (in the time or space domain) potentially requires that error covariance is taken into account.

To provide a practical solution to this problem, we generate ensemble members which incorporate the spatial and temporal covariance structure of the residuals. These ensembles can be easily averaged over any larger area and once averaged, they provide a predictive spread that is representative of the aggregated error. In order to generate these ensembles, we present hereafter a spatial autoregressive (SAR) noise model (Cressie and Wikle, 2011) which aims at reproducing the spatial and temporal autocorrelation structure found in the empirical residuals (ε). The SAR model is used to generate random realizations of these residuals (hereafter noted $\hat{\varepsilon}$) which have a spatial and temporal autocorrelation structure that is comparable to that of the empirical residuals (ε). De-seasonalized ensemble members ($GRACE_{REC}$) are obtained by combining the monthly water storage predictions (from Eq. 6) with the randomly generated residuals $\hat{\varepsilon}$.

$$\text{GRACE}_{\text{REC}}(\text{t}_\text{m}) = \beta \cdot deseas\big(\text{TWS}(\text{t}_{m})\big) + \hat{\varepsilon}(t_m) \quad (8)$$

Supprimé: t

2.4.2 Generation of random residuals

In the SAR model (Cressie and Wikle, 2011), residuals ($\hat{\varepsilon}(t_m)$, hereafter noted $\hat{\varepsilon}_{t_m}$) at a given monthly time step are represented as the sum of: 1) the product of the residual of the antecedent month ($\hat{\varepsilon}_{t_m-1}$) with a local (mascon-specific) autoregressive parameter (φ) and 2) spatially auto-correlated innovations (η) that are randomly generated from a multivariate Gaussian with zero mean and covariance matrix $\mathbf{Q_n}$:

$$\begin{bmatrix} \hat{\varepsilon}_{t_m}(m_1) \\ \vdots \\ \hat{\varepsilon}_{t_m}(m_n) \end{bmatrix} = \begin{bmatrix} \varphi(m_1) \cdot \hat{\varepsilon}_{t_m-1}(m_1) \\ \vdots \\ \varphi(m_n) \cdot \hat{\varepsilon}_{t_m-1}(m_n) \end{bmatrix} + \begin{bmatrix} \eta(m_1) \\ \vdots \\ \eta(m_n) \end{bmatrix} \quad (9)$$

where $m_{1,\dots,n}$ corresponds to the mascon index and squared brackets indicate a $n \times 1$ vector. An equivalent vector notation yields:

$$\hat{\boldsymbol{\varepsilon}}_{\boldsymbol{t_m}} = \boldsymbol{\varphi} \circ \hat{\boldsymbol{\varepsilon}}_{\boldsymbol{t_m-1}} + \boldsymbol{\eta}, \qquad \boldsymbol{\eta} \sim iid\ Gau(0, \mathbf{Q_n}) \quad (10)$$

where $\hat{\boldsymbol{\varepsilon}}_{\boldsymbol{t_m}}$, $\hat{\boldsymbol{\varepsilon}}_{\boldsymbol{t_m-1}}$, $\boldsymbol{\varphi}$ and $\boldsymbol{\eta}$ are $n \times 1$ vectors, $\mathbf{Q_n}$ is a $n \times n$ spatial covariance matrix and $\circ$ denotes the Hadamard product (i.e. pair-wise multiplication).

The local autoregressive parameters $\varphi(m_1, \dots, m_n)$ are estimated at each mascon from the lag-1 temporal autocorrelation of the empirical residuals (ε) (φ illustrated in Fig 2c) (Wilks, 2011). To estimate the spatial covariance matrix of the innovations ($\mathbf{Q_n}$), we employ the following procedure. First, an isotropic exponential decay autocorrelation function (Eq. 11) is fitted at each individual mascon (Fig 3a, b) to represent the spatial autocorrelation (AC) of the empirical residuals, such that:

$$AC(d) = e^{-\frac{d}{k}} \quad (11)$$

where d is the distance and k is the parameter to fit. Locations with high (low) values of k (Fig 3c) indicate regions where the residuals have a strong (weak) spatial autocorrelation. The calibrated AC

Supprimé: t

Supprimé: antecedent

Supprimé: t

Supprimé: t

Supprimé: t

Supprimé: follow

functions are then used to construct the spatial autocorrelation matrix $\mathbf{P_n}$ which approximates the structure of the spatial autocorrelation matrix of the empirical residuals. From this, the covariance matrix for the innovations is obtained by definition as:

$$\mathbf{Q_n} = \mathrm{diag}(\boldsymbol{\sigma_\eta})\, \mathbf{P_n}\, \mathrm{diag}(\boldsymbol{\sigma_\eta}) \tag{12}$$

where $\boldsymbol{\sigma_\eta}$ is a $n \times 1$ vector containing the standard deviation of the innovations at each mascon estimated from (Cressie and Wikle, 2011):

$$\boldsymbol{\sigma_\eta} = \boldsymbol{\sigma_\varepsilon} \circ \sqrt{1 - \boldsymbol{\varphi}^2} \tag{13}$$

where $\boldsymbol{\sigma_\varepsilon}$ is the empirical standard error of each mascon (Eq. 7, Fig 2a). The multiplication with $\sqrt{1 - \boldsymbol{\varphi}^2}$ scales the empirical standard error under the assumption of an autoregressive process of order 1 (Cressie and Wikle, 2011). This accounts for the fact that the variance of an autoregressive process ($\boldsymbol{\sigma_\varepsilon}$) is larger than that of the driving white noise process ($\boldsymbol{\sigma_\eta}$). In the special case where the first residual in Eq. (10) ($\hat{\boldsymbol{\varepsilon}}_{t_m}$ at $t_m = 1$) is generated and $\hat{\boldsymbol{\varepsilon}}_{t_m - 1}$ does not exist yet, the multiplication with $\sqrt{1 - \boldsymbol{\varphi}^2}$ is not necessary and the following formulations are used instead of Eq. (10) and (12):

$$\hat{\boldsymbol{\varepsilon}}_{\mathbf{1}} = \boldsymbol{\eta}, \qquad \boldsymbol{\eta} \sim iid\ Gau(0, \mathbf{Q'}_{\boldsymbol{n}}) \tag{14}$$

$$\mathbf{Q'}_{\boldsymbol{n}} = \mathrm{diag}(\boldsymbol{\sigma_\varepsilon}) \cdot \mathbf{P_n} \cdot\ \mathrm{diag}(\boldsymbol{\sigma_\varepsilon}) \tag{15}$$

To summarize, a first residual is generated with Eq. (14) and subsequent residuals are generated from Eq. (10).

As mentioned in section 2.3, the Markov Chain Monte Carlo (MCMC) procedure for model parameter estimation additionally provides a distribution of equally acceptable model parameters (a, b and β). Each parameter set provides one ensemble member for which the entire procedure described here is repeated.

Thus, ensemble members combine 1) a model parameter uncertainty arising from the distribution of calibrated model parameters and 2) an estimate of the predictive uncertainty. Here, we provide one hundred randomly sampled ensemble members. This number was chosen as a compromise between the size of the final dataset and the minimum number of ensemble members required to derive a reasonable estimate of the 90% confidence interval.

Supprimé: structural

2.4.3 Evaluation of ensemble members

The result of the above-described procedure is briefly illustrated and evaluated in Fig. 4. For illustration, Fig. 4a shows the empirical residuals (ε) for the month of April 2002 and Fig. 4b shows one instance of the randomly generated residuals ($\hat{\varepsilon}$). As expected, both the empirical and the randomly generated residuals exhibit spatial autocorrelation. The generated residuals also have approximately the same variance (Fig. 4c) and lag-1 temporal autocorrelation (Fig. 4d) as that of the empirical residuals. The confidence intervals derived at a regional or basin-scale level reliably cover the actual GRACE-based regional average which was the initial motivation for the presented approach (illustrated for the Mississippi basin in Fig. 4e). We evaluate the overall *reliability* of the ensemble hindcast for regional averages over 90 large (>500'000 km^2) river basins using a rank histogram (or Talagrand diagram) (Fig. 4f). In the ideal case (*perfect reliability*), the observed TWS ranks lower than the P^{th} percentile of the reconstruction only P percent of the time (for instance, GRACE observations should be lower than the 5th percentile of the reconstruction only 5% of the time). According to this first order metric (see e.g. Hamill, 2001 for a discussion), we conclude that regional averages of the ensemble members provide *reliable* forecasts (Fig. 4f), with only a minor tendency to miss extreme positive TWS anomalies.

The presented method represents one amongst many possible approaches to the generation of ensemble members. This method has the advantage of reflecting the uncertainty of the reconstruction (compared to GRACE measurements) and mimics the empirical spatiotemporal auto-correlation structure of the errors while only requiring a minimal degree of model complexity and parameterization. We note that while the SAR model also represents errors coming from the GRACE solution itself, it does not include any anisotropic error structure (e.g. due to striping) due to the isotropic nature of Eq. (11). The uncertainty

related to the choice of the input precipitation or training GRACE dataset can be explored independently by comparing the six different versions of GRACE-REC (see Table 3).

Finally, we note that our modelling approach could in principle be evaluated with a cross-validation experiment, using only a subset of the data to calibrate the model parameters and then evaluate the performance against the other unused data (as done in Humphrey et al., 2017). However, this would go beyond the scope and objective of this paper which is to document the generation of the GRACE-REC product. We prefer to evaluate the ability of the final product to extrapolate beyond the model calibration period in later sections by comparing the model predictions with fully independent datasets (Sections 4.3 to 4.5).

Supprimé: “

Supprimé: ”

3 Product description

3.1 Definition of GRACE-REC TWS datasets

The GRACE-REC data provide de-seasonalized terrestrial water storage (TWS) anomalies in units of millimetres of water (kg/m^2) (Eq. 8). Thus, GRACE-REC does not include a reconstructed seasonal TWS cycle. Because some applications also require the seasonal signals, we provide the GRACE-based TWS seasonal cycle (Humphrey et al., 2017) which can directly be added to the GRACE-REC TWS anomalies if needed. As a caveat, note that this GRACE-based TWS seasonal cycle is kept constant over time, which might potentially be unrealistic (Hamlington et al., 2019).

3.2 Monthly products with ensemble members

Using two different training GRACE datasets (Table 1) and three different precipitation forcing datasets (Table 2), we produce a total of six different GRACE-REC datasets with 100 ensemble members each. For convenience, we also provide smaller summary files which only contain the ensemble mean and 90% confidence interval.

3.3 Daily products

For the daily TWS reconstructions, we only provide the ensemble mean of each GRACE-REC product in order to limit the data size. This ensemble mean is based on ensemble members which sample the

parameter uncertainty only (Section 2.3.2). The reason for this is that no SAR model (Section 2.4.2) can be reliably calibrated at the daily resolution as the two training GRACE datasets have monthly resolution. The format is identical to that of the monthly data (Table 3).

3.4 Global land averages

For global-scale applications, we provide global averages of the TWS time series. Global averages are weighted by mascon area and include all land mascons with or without Greenland and Antarctica (both options are available). This format is especially suited for sea level and global water budget studies and units are gigatons of water. To convert gigatons back to millimetres of global land water, total land area values of 148'940'000 km^2 and 132'773'914 km^2 can be used for each option respectively. The evaluation of global means in Sections 4.1.2 and 4.3 can guide the choice between the different versions of GRACE-REC.

3.5 Interpretation of multi-decadal trends

Supprimé: Important limitations and caveats

Although linear trends are removed during model calibration (Eq. 6), potential TWS trends caused by decadal variability and long-term changes in precipitation are not removed from the final dataset (Eq. 8) and can be substantial. By definition, any trend found in the reconstructed TWS products is caused by a trend in the underlying precipitation forcing (since the time-varying residence time is using de-trended temperature and there is no limit to storage capacity). Thus the reconstructed TWS trends mainly depend on the trends initially present in the driving precipitation data (see section 4.1.2 for an example at global scale).

With these elements in mind, it should be clear that there will be differences between the trends found in GRACE and the trends found in the reconstruction. Such discrepancies are expected because the reconstruction does not represent several sources of long-term changes in TWS, including for instance, land ice melt, dams, anthropogenic water depletion (Reager et al., 2016;Felfelani et al., 2017;Rodell et al., 2018) or long-term changes in evaporative demand. Consequently, trends in GRACE-REC cannot be directly evaluated against the trends from GRACE itself. Thus, when we compute trends over the period 2003-2014 (Supplementary Information, Figures S2 & S3), we find that reconstructed trends are

Supprimé: is

consistent with GRACE trends only over certain regions, likely due to the reasons mentioned above (linear trends simulated by the WRR2 models are also shown in Figure S4).

As illustrated in Humphrey et al. (2017), the reconstruction can be used to remove the precipitation-driven variability from the original GRACE time series in order to better isolate and quantify other sources of long-term changes (such as anthropogenic impacts). However, users interested in computing long-term TWS trends from this dataset should always proceed with caution as the dataset was not evaluated for trends. For regional analyses, we recommend to use the model ensembles to obtain a range of possible trends and thus better assess the uncertainty. More generally, we highlight that the quality of the reconstruction is strongly dependent on the quality of the input precipitation forcing and on the adequateness of an exponential decay model for representing water storage behaviour. For instance, routing of water through the river system is not represented and might be important over certain regions. Section 4.1 provides global maps of model performance that can guide regional applications.

Supprimé: these

Supprimé: .

4 Product evaluation

4.1 Comparison with de-seasonalized monthly GRACE

4.1.1 Mascon scale

In this section, the ensemble mean of GRACE-REC is compared against GRACE observations. Note that this does not constitute an independent evaluation because GRACE-REC is calibrated with GRACE data (comparisons with independent sources are provided in sections 4.3 to 4.5). We evaluate model performance with the Pearson correlation coefficient (Fig. 5) and the Nash-Sutcliffe Efficiency (Fig. 6). Model performance is highest especially in regions with dense meteorological observing systems (e.g. Europe, Western Russia, North America, India, Australia) where we expect precipitation datasets to have the highest accuracy. Over South America and Central Africa, the performance of the century-long reconstruction (GSWP3 based products, Fig. 5c-d and 6c-d) is slightly inferior to that of multi-source and reanalysis precipitation datasets such as MSWEP and ERA5. Interestingly, there is no clear difference in performance when GRACE-REC is calibrated with the 3° JPL Mascons (left column) or the 1° GSFC Mascons (right column). We conclude that in terms of model performance, the choice of the GRACE

Supprimé: reanalysis-based precipitation

Supprimé: ERA-Interim

Supprimé: e

Supprimé: f

Supprimé: e

Supprimé: f

Supprimé: GSWP3

Supprimé: MSWEP

Supprimé: (note that GSWP3 is bias-corrected with GPCP, which is using both station and satellite data)

product used to calibrate GRACE-REC is of secondary importance compared to the accuracy of the input precipitation datasets.

We compare these performance metrics with the scores obtained by hydrological models and land surface models of the Water Resources Reanalysis version 2 (WRR2) (Schellekens et al., 2017;Dutra et al., 2017), which were also forced with MSWEP precipitation. Compared to the simple modelling approach used in GRACE-REC, WRR2 models are forced with additional meteorological information (such as radiation and humidity), were calibrated using various data streams, sometimes including GRACE observations (Dutra et al., 2017;Decharme et al., 2011;Decharme et al., 2012;Vergnes et al., 2014;Decharme et al., 2016;Krinner et al., 2005;de Rosnay et al., 2002;Van Der Knijff et al., 2010;Döll et al., 2009;Sutanudjaja et al., 2011, 2014;van Beek and Bierkens, 2008;van Beek et al., 2011;Wada et al., 2011;Wada et al., 2014;van Dijk et al., 2013;van Dijk et al., 2014), and are potentially able to resolve more complex processes that are relevant for TWS, such as snow dynamics, the effect of vegetation phenology on evapotranspiration, and runoff routing through the river system. We calculate TWS in WRR2 models by summing over all simulated water reservoirs (this includes soil moisture, snow, groundwater and surface waters whenever these are represented in the models). It is important to underline that unlike WRR2 models, GRACE-REC is directly calibrated to reproduce GRACE observations. Therefore, GRACE-REC should be interpreted here as a benchmark, indicative of the performance that is at least achievable for a given precipitation dataset. In terms of Nash-Sutcliffe efficiency, GRACE-REC often obtains better scores than the WRR2 models (Fig 7a). This is because the reconstruction better fits the local amplitude and variance of the observed TWS signal, as already diagnosed in previous work (Humphrey et al., 2017). We note that the reconstructions driven with ERA5 precipitation are most often superior to those driven with the other two precipitation datasets.

Supprimé: MSWEP

Supprimé: systematically

Supprimé: (note WRR2 is driven with MSWEP as well)

4.1.2 Global scale

Global averages of all GRACE-REC products are illustrated in Fig. 8a. Differences caused by different precipitation forcing datasets are much greater than the differences related to different GRACE training datasets. This is particularly true for long-term (> 20 years) trends as we find that, over the overlapping period 1979-2014, the two MSWEP-based products both produce a positive climate-driven TWS trend

while GSWP3-based and ERA5-based products yield a negative TWS trend. As mentioned above (see section 3.5), discrepancies in long-term trends in GRACE-REC largely depend on the trends initially present in the driving precipitation data and also do not incorporate effects such as groundwater depletion or potential long-term changes in evaporative demand.

Comparisons with the de-trended GRACE global average are shown in Fig. 8b-c. We find that all GRACE-REC products produce a very similar inter-annual variability at the global scale and compare well against actual global mean GRACE, this without applying any global constraint to the locally calibrated statistical model. Correlations between global means of GRACE-REC and global means of GRACE are larger than 0.75 (Fig 9a) (evaluated over the common period 2003-2014). Compared to global means from the WRR2 models, GRACE-REC is on average better correlated (Fig. 9a) to the observed GRACE global mean and has a lower root mean square error (Fig. 9b), regardless of the GRACE dataset used for evaluation.

4.2 Comparison with de-seasonalized daily GRACE

We compare the daily GRACE-REC products with a Kalman smoothed daily GRACE solution named JTSG-Grace2018 (Kurtenbach et al., 2012;Mayer-Gürr et al., 2018). While this daily GRACE solution contains significant information on the sub-monthly variability of TWS, the increased temporal resolution is at the cost of spatial resolution, which is in the order of 500km for this particular product (note that the solution is also correlated in time as a result of the Kalman smoothing). As illustrated in Figure 10a, there can be a good agreement between GRACE-REC and JTSG-Grace2018 for submonthly variability when daily averages are computed over large regions (here the Mississippi basin). Figure 10b-c provides a summary of the agreement between GRACE-REC and JTSG-Grace2018 at daily scale, as well as a comparison with the performance of WRR2 models. Due to the coarse resolution of the JTSG-Grace2018 product, the comparison (Fig. 10b-c) is conducted at a spatial resolution of 5°. We find that, even though the performance of all products is lower than at monthly resolution, the GRACE-REC products agree on average as well or better with JTSG-Grace2018 than most models of the WRR2 ensemble.

Supprimé: We conclude

Supprimé: that

Supprimé: should be interpreted with the awareness that reconstructed TWS trends strongly

Supprimé: Note that trends in GRACE-REC cannot be directly evaluated against the trends from GRACE itself. This is because GRACE-REC only represents precipitation-driven effects, whereas GRACE observations also include effects of groundwater depletion, dams and glacier melt (Reager et al., 2016;Felfelani et al., 2017;Rodell et al., 2018) as well as potential effects of climate change on evaporative demand.

Supprimé: and

Supprimé: in general

Supprimé: ITSG2018

Supprimé: ITSG2018

Supprimé: ITSG2018

Supprimé: ITSG2018

Supprimé: ITSG2018

4.3 Comparison with the de-seasonalized and de-trended sea level budget

Together with changes in ocean heat content, changes in the amount of water stored on land are responsible for a large fraction of the year-to-year variability in global mean sea level (Boening et al., 2012;Cazenave et al., 2014;Cazenave, 2018). Because changes in land water storage result in opposite changes in ocean mass, the sea level budget provides an independent mean of evaluating various estimates of global mean TWS variability. Here we assess the ability of terrestrial water storage products (GRACE, GRACE-REC, and the WRR2 models) to close the sea level budget at the inter-annual time scale. We use de-seasonalized and de-trended global mean sea level (GMSL) from satellite altimetry (Beckley et al., 2017) and steric height estimates ($GMSL_{steric}$) based on observations of Argo floats (Roemmich and Gilson, 2009;Llovel et al., 2014). From the sea level budget, we obtain an estimate of inter-annual changes in ocean mass (Eq. 16, black line in Fig. 11a) which we compare against global mean TWS estimates. We use this budget-based ocean mass to provide an independent evaluation of all TWS products (i.e. not based on any GRACE data), although GRACE-based ocean mass is obviously also available since 2002 (e.g. Watkins et al., 2015). Greenland and Antarctica are excluded from the TWS averages to enable a consistent comparison among all products (hydrological models typically do not represent these regions).

$$GMSL_{ocean\ mass} = GMSL - GMSL_{steric} \quad (16)$$

We find that, although all considered products are significantly correlated with the budget-based ocean mass ($GMSL_{ocean\ mass}$), GRACE and GRACE-REC estimates are clearly better correlated and yield a lower root mean square error (Fig. 11b-c). Surprisingly, GRACE-REC products also yield better results than the two original GRACE datasets (JPL and GSFC). We hypothesize that this might occur because the global mean GRACE TWS is more susceptible to non-compensating continental-scale errors (e.g. caused by errors in low degree spherical harmonics or residual longitudinal stripes) compared to climate-driven reconstructions which yield smoother global averages (as seen in Fig. 8b,c).

4.4 Comparison with de-seasonalized basin-scale water balance

Over moderately large river basins (>100'000km^2), TWS changes can be estimated by combining streamflow measurements with moisture fluxes from an observation-assimilating atmospheric reanalysis system (Oki et al., 1995;Seneviratne et al., 2004). This approach provides relatively independent estimates of TWS changes over large basins which has been used to evaluate distributed hydrological models and land surface models. Here, we aim to use such estimates to evaluate the quality of the reconstruction also during the period where no GRACE data is available (i.e. prior to 2002).

We evaluate TWS products using a recently updated basin-scale water balance dataset (BSWB) (Hirschi and Seneviratne, 2017) which covers 341 catchments and is based on ERA-Interim reanalysis data (Dee et al., 2011) and runoff observations from the Global Runoff Data Centre (GRDC). The temporal coverage of BSWB estimates at each river basin thus depends on the availability of runoff data and does not always cover the GRACE time period. As a caveat, we note that BSWB should not be viewed as entirely independent from WRR2 models neither as a ground truth. This is because moisture fluxes from ERA-Interim are not only influenced by the assimilated atmospheric profile information but are also dependent on the underlying land surface model (TESSEL), which is similar to WRR2 models in many aspects. All WRR2 models also used ERA-Interim as forcing data for all meteorological variables except for precipitation.

As illustrated in Fig 12a for the Ob basin, we find that the reconstructed TWS compares relatively well with BSWB estimates. Overall, all TWS products considered here (including the GRACE data itself) seem to compare relatively well with BSWB (Fig 12b-c). We note that GRACE-REC products calibrated on GSFC seem to compare slightly better with BSWB than the JPL-based products. This might be because of the higher spatial sampling of the GSFC mascons (1° instead of 3° for JPL) which might enable a better separation between mass changes located inside or outside the river basin boundaries. This mainly occurs because the meteorological forcing is aggregated at a resolution of 1° in the case of GSFC-based products, allowing the GSFC reconstructions to provide a slightly more localized signal.

Supprimé: Similarly, the JPL-MSWEP and GSFC-MSWEP reconstructions use ERA-Interim air temperature, while JPL-ERAI and GSFC-ERAI reconstructions use both ERA-Interim precipitation and air temperature.

Supprimé: equally

Supprimé: GRACE GSFC data and

Supprimé: resolution

Supprimé: .

4.5 Comparison with annual streamflow measurements

In this section, we compare reconstructed TWS against streamflow observations over the period 1901 to 2010. Streamflow and TWS of course represent different variables with different units, however, we expect that their temporal dynamics will correlate at the yearly scale, as illustrated for the river Thames in Fig 13a-b. Because observed streamflow is one of the few water cycle variables available prior to 1980, it provides an independent and useful means of evaluating the century-long reconstruction. We use streamflow observations collected by the Global Streamflow Indices and Metadata Archive (GSIM) (Do et al., 2018;Gudmundsson et al., 2018). From the 30'959 available stations, we keep stations with basin size smaller than 10'000 km^2 and with at least 10 years of available data (discarding any year where less than 50% of the daily values were available to compute the yearly mean), leaving 12'496 stations for analysis. The reason for focusing on small basins is that a much larger number of them is available in the early century (compared to the number of large basins, which are the focus of section 4.4). We note that the unavoidable mismatch in resolution between large-scale mass changes and local catchment runoff dynamics is to some extent alleviated by the spatial coherence of yearly anomalies in weather patterns.

We find that TWS anomalies from both WRR2 models and GRACE-REC compare well with yearly streamflow variability over the period 1980-2010 (Fig. 13c). Reconstructions based on the GSFC products tend to perform slightly better, again likely because of their higher spatial sampling (1°) compared to the JPL-based reconstructions (3°). When evaluating the century-long reconstruction (GSWP3-driven products), we find that the correlation between yearly TWS anomalies and yearly runoff only slightly degrades for the earliest time period (1901-1940) but is otherwise relatively stable over time (Fig. 13d). This indicates that, even though GRACE-REC was calibrated over the years 2002-2016, the model is still able to reproduce past water cycle variability and does not overfit to the period of the GRACE mission. In addition, we note that the quality of the century-long reconstruction is of course dependent on the accuracy of the GSWP3 precipitation and temperature forcing, which likely degrades towards the beginning of the century as less observations are available.

Supprimé: resolution

5 Data availability

The presented dataset is publicly available (https://doi.org/10.6084/m9.figshare.7670849) and updates of the two reconstructions driven by ERA5 will be published when needed. We note that because including additional GRACE months only barely improves the quality of the model fit, no systematic re-calibration of the models is planned at this stage. The data can be freely used provided this paper is acknowledged.

6 Conclusions

We present a statistical reconstruction of climate-driven terrestrial water storage changes at daily and monthly resolution in six different configurations which cover three different time periods (Table 3). We evaluate the performance of this reconstruction and show that its overall accuracy is reasonable compared to other estimates of TWS variability available from global hydrological models. We also highlight the versatility and robustness of our approach by comparing our estimates with independent observations of Earth system variables outside of the calibration period.

7 Author contribution

VH and LG developed the approach. VH performed the analyses, produced the dataset and wrote the manuscript with feedback from LG.

8 Competing interests

The authors declare that they have no conflict of interest.

9 Acknowledgements

This research was funded by the European Research Council DROUGHT-HEAT project (contract 617518) and by the Swiss National Science Foundation (P400P2_180784). We thank Prof. Dr. Sonia Seneviratne for critical feedback and support of this work. We thank Prof. Dr. Hyungjun Kim for developing the GSWP3 forcing and providing us with early access to the data

Supprimé:

(https://doi.org/10.20783/DIAS.501). We thank Dr. Richard Wartenburger for technical support. Model developers and data providers are also gratefully acknowledged for sharing their data: GRACE JPL Mascons (https://grace.jpl.nasa.gov/data/get-data/jpl_global_mascons/), GRACE GSFC (https://neptune.gsfc.nasa.gov/gngphys/index.php?section=470), MSWEP V2 (http://www.gloh2o.org/), ERA5 (https://cds.climate.copernicus.eu/#!/search?text=ERA5&type=dataset), JTSG-Grace2018 (http://icgem.gfz-potsdam.de/series), NASA Sea Level Change Portal (https://sealevel.nasa.gov/), BSWB (doi:10.5905/ethz-1007-82), GRDC Reference Dataset (https://www.bafg.de/GRDC), GSIM (https://doi.org/10.1594/PANGAEA.887477), WRR2 (http://wci.earth2observe.eu/thredds/catalog-earth2observe-model-wrr2.html) and the Earth2Observe project (http://www.earth2observe.eu/).

Supprimé: -Interim

Supprimé: http://apps.ecmwf.int/datasets/data/ interim-full-daily

Supprimé: ITSG2018

References

A, G., Wahr, J., and Zhong, S.: Computations of the viscoelastic response of a 3-D compressible Earth to surface loading: an application to Glacial Isostatic Adjustment in Antarctica and Canada, Geophysical Journal International, 192, 557-572, 10.1093/gji/ggs030, 2013.

Adhikari, S., and Ivins, E. R.: Climate-driven polar motion: 2003-2015, Science Advances, 2, 10.1126/sciadv.1501693, 2016.

Anderegg, W. R. L., Konings, A. G., Trugman, A. T., Yu, K., Bowling, D. R., Gabbitas, R., Karp, D. S., Pacala, S., Sperry, J. S., Sulman, B. N., and Zenes, N.: Hydraulic diversity of forests regulates ecosystem resilience during drought, Nature, 561, 538-541, 10.1038/s41586-018-0539-7, 2018.

Andrew, R., Guan, H., and Batelaan, O.: Estimation of GRACE water storage components by temporal decomposition, Journal of Hydrology, 552, 341-350, 10.1016/j.jhydrol.2017.06.016, 2017.

Beck, H. E., van Dijk, A. I. J. M., Levizzani, V., Schellekens, J., Miralles, D. G., Martens, B., and de Roo, A.: MSWEP: 3-hourly 0.25 degrees global gridded precipitation (1979-2015) by merging gauge, satellite, and reanalysis data, Hydrology and Earth System Sciences, 21, 589-615, 10.5194/hess-21-589-2017, 2017.

Beck, H. E., Wood, E. F., Pan, M., Fisher, C. K., Miralles, D. G., van Dijk, A. I. J. M., McVicar, T. R., and Adler, R. F.: MSWEP V2 global 3-hourly 0.1° precipitation: methodology and quantitative assessment, Bulletin of the American Meteorological Society, 10.1175/bams-d-17-0138.1, 2018.

Beckley, B. D., Callahan, P. S., Hancock, D. W., Mitchum, G. T., and Ray, R. D.: On the "Cal-Mode" Correction to TOPEX Satellite Altimetry and Its Effect on the Global Mean Sea Level Time Series, Journal of Geophysical Research: Oceans, 122, 8371-8384, 10.1002/2017jc013090, 2017.

Beguería, S., Vicente-Serrano, S. M., Reig, F., and Latorre, B.: Standardized precipitation evapotranspiration index (SPEI) revisited: parameter fitting, evapotranspiration models, tools, datasets and drought monitoring, International Journal of Climatology, 34, 3001-3023, 10.1002/joc.3887, 2014.

Bento, V. A., Gouveia, C. M., DaCamara, C. C., and Trigo, I. F.: A climatological assessment of drought impact on vegetation health index, Agr Forest Meteorol, 259, 286-295, 10.1016/j.agrformet.2018.05.014, 2018.

Beven, K. J.: Rainfall-Runoff Modelling: The Primer, 2nd ed., John Wiley & Sons, Chichester, 2012.

Bevington, P. R., and Robinson, D. K.: Data reduction and error analysis for the physical sciences, Third edition ed., McGraw-Hill, Boston, 320 S. pp., 2003.

Boening, C., Willis, J. K., Landerer, F. W., Nerem, R. S., and Fasullo, J.: The 2011 La Nina: So strong, the oceans fell, Geophysical Research Letters, 39, 2012.

Cazenave, A., Dieng, H. B., Meyssignac, B., von Schuckmann, K., Decharme, B., and Berthier, E.: The rate of sea-level rise, Nature Climate Change, 4, 358-361, 10.1038/nclimate2159, 2014.

Cazenave, A.: Global sea-level budget 1993–present, Earth Syst Sci Data, 10, 1551-1590, 10.5194/essd-10-1551-2018, 2018.

Chambers, D. P., Cazenave, A., Champollion, N., Dieng, H., Llovel, W., Forsberg, R., von Schuckmann, K., and Wada, Y.: Evaluation of the Global Mean Sea Level Budget between 1993 and 2014, Surv Geophys, 10.1007/s10712-016-9381-3, 2016.

Chao, B. F., Wu, Y. H., and Li, Y. S.: Impact of Artificial Reservoir Water Impoundment on Global Sea Level, Science, 320, 212-214, 10.1126/science.1154580, 2008.
Chen, J., Famiglietti, J. S., Scanlon, B. R., and Rodell, M.: Groundwater storage changes: present status from GRACE observations, Surv Geophys, 37, 397-417, 10.1007/s10712-015-9332-4, 2016.
Cheng, L., Trenberth, K. E., Fasullo, J., Boyer, T., Abraham, J., and Zhu, J.: Improved estimates of ocean heat content from 1960 to 2015, Science Advances, 3, e1601545, 10.1126/sciadv.1601545, 2017.
Compo, G. P., Whitaker, J. S., Sardeshmukh, P. D., Matsui, N., Allan, R. J., Yin, X., Gleason, B. E., Vose, R. S., Rutledge, G., Bessemoulin, P., Brönnimann, S., Brunet, M., Crouthamel, R. I., Grant, A. N., Groisman, P. Y., Jones, P. D., Kruk, M. C., Kruger, A. C., Marshall, G. J., Maugeri, M., Mok, H. Y., Nordli, Ø., Ross, T. F., Trigo, R. M., Wang, X. L., Woodruff, S. D., and Worley, S. J.: The Twentieth Century Reanalysis Project, Quarterly Journal of the Royal Meteorological Society, 137, 1-28, 10.1002/qj.776, 2011.
Cressie, N. A. C., and Wikle, C. K.: Statistics for spatio-temporal data, Wiley series in probability and statistics, Wiley, Hoboken, N.J., 588 S. pp., 2011.
D'Orangeville, L., Maxwell, J., Kneeshaw, D., Pederson, N., Duchesne, L., Logan, T., Houle, D., Arseneault, D., Beier, C. M., Bishop, D. A., Druckenbrod, D., Fraver, S., Girard, F., Halman, J., Hansen, C., Hart, J. L., Hartmann, H., Kaye, M., Leblanc, D., Manzoni, S., Ouimet, R., Rayback, S., Rollinson, C. R., and Phillips, R. P.: Drought timing and local climate determine the sensitivity of eastern temperate forests to drought, Global Change Biology, 24, 2339-2351, 10.1111/gcb.14096, 2018.
Dai, A., and Zhao, T.: Uncertainties in historical changes and future projections of drought. Part I: estimates of historical drought changes, Climatic Change, 144, 519-533, 10.1007/s10584-016-1705-2, 2016.
de Rosnay, P., Polcher, J., Bruen, M., and Laval, K.: Impact of a physically based soil water flow and soil-plant interaction representation for modeling large-scale land surface processes, J Geophys Res-Atmos, 107, 2002.
Decharme, B., Boone, A., Delire, C., and Noilhan, J.: Local evaluation of the Interaction between Soil Biosphere Atmosphere soil multilayer diffusion scheme using four pedotransfer functions, J Geophys Res-Atmos, 116, 2011.
Decharme, B., Alkama, R., Papa, F., Faroux, S., Douville, H., and Prigent, C.: Global off-line evaluation of the ISBA-TRIP flood model, Climate Dynamics, 38, 1389-1412, 2012.
Decharme, B., Brun, E., Boone, A., Delire, C., Le Moigne, P., and Morin, S.: Impacts of snow and organic soils parameterization on northern Eurasian soil temperature profiles simulated by the ISBA land surface model, Cryosphere, 10, 853-877, 2016.
Dee, D. P., Uppala, S. M., Simmons, A. J., Berrisford, P., Poli, P., Kobayashi, S., Andrae, U., Balmaseda, M. A., Balsamo, G., Bauer, P., Bechtold, P., Beljaars, A. C. M., van de Berg, L., Bidlot, J., Bormann, N., Delsol, C., Dragani, R., Fuentes, M., Geer, A. J., Haimberger, L., Healy, S. B., Hersbach, H., Hólm, E. V., Isaksen, L., Kållberg, P., Köhler, M., Matricardi, M., McNally, A. P., Monge-Sanz, B. M., Morcrette, J. J., Park, B. K., Peubey, C., de Rosnay, P., Tavolato, C., Thépaut, J. N., and Vitart, F.: The ERA-Interim reanalysis: configuration and performance of the data assimilation system, Quarterly Journal of the Royal Meteorological Society, 137, 553-597, 10.1002/qj.828, 2011.
Dieng, H. B., Cazenave, A., Meyssignac, B., and Ablain, M.: New estimate of the current rate of sea level rise from a sea level budget approach, Geophysical Research Letters, 44, 3744-3751, 10.1002/2017gl073308, 2017.
Dill, R., and Dobslaw, H.: Numerical simulations of global-scale high-resolution hydrological crustal deformations, Journal of Geophysical Research: Solid Earth, 118, 5008-5017, 10.1002/jgrb.50353, 2013.
Do, H. X., Gudmundsson, L., Leonard, M., and Westra, S.: The Global Streamflow Indices and Metadata Archive (GSIM) – Part 1: The production of a daily streamflow archive and metadata, Earth Syst Sci Data, 10, 765-785, 10.5194/essd-10-765-2018, 2018.
Döll, P., Fiedler, K., and Zhang, J.: Global-scale analysis of river flow alterations due to water withdrawals and reservoirs, Hydrology and Earth System Sciences, 13, 2413-2432, 2009.
Dutra, E., Balsamo, G., Calvet, J., Munier, S., Burke, S., Fink, G., van Dijk, A., Martinez-de la Torre, A., van Beek, R., and de Roo, A.: Report on the improved Water Resources Reanalysis. EartH2Observe, Report No.: 5.2., 94 pp, 2017.
Eicker, A., Forootan, E., Springer, A., Longuevergne, L., and Kusche, J.: Does GRACE see the terrestrial water cycle "intensifying"?, J Geophys Res-Atmos, 121, 733-745, 2016.
Fasullo, J. T., Lawrence, D. M., and Swenson, S. C.: Are GRACE-era Terrestrial Water Trends Driven by Anthropogenic Climate Change?, Adv Meteorol, 2016.
Felfelani, F., Wada, Y., Longuevergne, L., and Pokhrel, Y. N.: Natural and human-induced terrestrial water storage change: A global analysis using hydrological models and GRACE, Journal of Hydrology, 553, 105-118, 10.1016/j.jhydrol.2017.07.048, 2017.
Frederikse, T., Jevrejeva, S., Riva, R. E. M., and Dangendorf, S.: A Consistent Sea-Level Reconstruction and Its Budget on Basin and Global Scales over 1958–2014, Journal of Climate, 31, 1267-1280, 10.1175/jcli-d-17-0502.1, 2018.
Gao, S., Liu, R., Zhou, T., Fang, W., Yi, C., Lu, R., Zhao, X., and Luo, H.: Dynamic responses of tree-ring growth to multiple dimensions of drought, Global Change Biology, 24, 5380-5390, 10.1111/gcb.14367, 2018.
Getirana, A., Kumar, S., Girotto, M., and Rodell, M.: Rivers and Floodplains as Key Components of Global Terrestrial Water Storage Variability, Geophysical Research Letters, 44, 10,359-310,368, 10.1002/2017gl074684, 2017.
Griffin, D., and Anchukaitis, K. J.: How unusual is the 2012-2014 California drought?, Geophysical Research Letters, 41, 9017-9023, 10.1002/2014gl062433, 2014.

Gudmundsson, L., Do, H. X., Leonard, M., and Westra, S.: The Global Streamflow Indices and Metadata Archive (GSIM) – Part 2: Quality control, time-series indices and homogeneity assessment, Earth Syst Sci Data, 10, 787-804, 10.5194/essd-10-787-2018, 2018.
Haario, H., Laine, M., Mira, A., and Saksman, E.: DRAM: Efficient adaptive MCMC, Statistics and Computing, 16, 339-354, 10.1007/s11222-006-9438-0, 2006.
Hamill, T. M.: Interpretation of Rank Histograms for Verifying Ensemble Forecasts, Mon Weather Rev, 129, 550-560, 10.1175/1520-0493(2001)129<0550:iorhfv>2.0.co;2, 2001.
Hamlington, B. D., Reager, J. T., Chandanpurkar, H., and Kim, K. Y.: Amplitude Modulation of Seasonal Variability in Terrestrial Water Storage, Geophysical Research Letters, 10.1029/2019gl082272, 2019.
Hanasaki, N., Yoshikawa, S., Pokhrel, Y., and Kanae, S.: A global hydrological simulation to specify the sources of water used by humans, Hydrology and Earth System Sciences, 22, 789-817, 10.5194/hess-22-789-2018, 2018.
Haslinger, K., and Blöschl, G.: Space-Time Patterns of Meteorological Drought Events in the European Greater Alpine Region Over the Past 210 Years, Water Resources Research, 53, 9807-9823, 10.1002/2017wr020797, 2017.
Heim, R. R.: A Comparison of the Early Twenty-First Century Drought in the United States to the 1930s and 1950s Drought Episodes, Bulletin of the American Meteorological Society, 98, 2579-2592, 10.1175/bams-d-16-0080.1, 2017.
Hersbach, H., and Dee, D.: ERA5 reanalysis is in production, ECMWF newsletter, 147(7), 2016.
Hirschi, M., and Seneviratne, S. I.: Basin-scale water-balance dataset (BSWB): an update, Earth Syst Sci Data, 9, 251-258, 10.5194/essd-9-251-2017, 2017.
Huang, M., Wang, X., Keenan, T. F., and Piao, S.: Drought timing influences the legacy of tree growth recovery, Global Change Biology, 24, 3546-3559, 10.1111/gcb.14294, 2018.
Humphrey, V.: Terrestrial water storage: large-scale variability and the global carbon cycle, Diss ETH 24696, Zürich, 156 pp., 2017.
Humphrey, V., Gudmundsson, L., and Seneviratne, S. I.: A global reconstruction of climate-driven subdecadal water storage variability, Geophysical Research Letters, 44, 2300-2309, 10.1002/2017GL072564, 2017.
Humphrey, V., Zscheischler, J., Ciais, P., Gudmundsson, L., Sitch, S., and Seneviratne, S. I.: Sensitivity of atmospheric CO2 growth rate to observed changes in terrestrial water storage, Nature, 560, 628-631, 10.1038/s41586-018-0424-4, 2018.
Jacob, T., Wahr, J., Pfeffer, W. T., and Swenson, S.: Recent contributions of glaciers and ice caps to sea level rise, Nature, 482, 514-518, 2012.
Khaki, M., Forootan, E., Kuhn, M., Awange, J., van Dijk, A. I. J. M., Schumacher, M., and Sharifi, M. A.: Determining water storage depletion within Iran by assimilating GRACE data into the W3RA hydrological model, Advances in Water Resources, 114, 1-18, 10.1016/j.advwatres.2018.02.008, 2018.
Kim, H. J.: Global Soil Wetness Project Phase 3 Atmospheric Boundary Counditions (Experiment 1), 10.20783/DIAS.501, 2017.
Krinner, G., Viovy, N., de Noblet-Ducoudre, N., Ogee, J., Polcher, J., Friedlingstein, P., Ciais, P., Sitch, S., and Prentice, I. C.: A dynamic global vegetation model for studies of the coupled atmosphere-biosphere system, Global Biogeochem Cy, 19, 2005.
Kurtenbach, E., Eicker, A., Mayer-Gürr, T., Holschneider, M., Hayn, M., Fuhrmann, M., and Kusche, J.: Improved daily GRACE gravity field solutions using a Kalman smoother, Journal of Geodynamics, 59-60, 39-48, 10.1016/j.jog.2012.02.006, 2012.
Kusche, J., Eicker, A., Forootan, E., Springer, A., and Longuevergne, L.: Mapping probabilities of extreme continental water storage changes from space gravimetry, Geophysical Research Letters, 43, 8026-8034, 10.1002/2016gl069538, 2016.
Llovel, W., Willis, J. K., Landerer, F. W., and Fukumori, I.: Deep-ocean contribution to sea level and energy budget not detectable over the past decade, Nature Climate Change, 4, 1031-1035, 10.1038/nclimate2387, 2014.
Luthcke, S. B., Sabaka, T. J., Loomis, B. D., Arendt, A. A., McCarthy, J. J., and Camp, J.: Antarctica, Greenland and Gulf of Alaska land-ice evolution from an iterated GRACE global mascon solution, Journal of Glaciology, 59, 613-631, 10.3189/2013JoG12J147, 2013.
Markonis, Y., Hanel, M., Máca, P., Kyselý, J., and Cook, E. R.: Persistent multi-scale fluctuations shift European hydroclimate to its millennial boundaries, Nature Communications, 9, 10.1038/s41467-018-04207-7, 2018.
Mayer-Gürr, T., Behzadpour, S., Ellmer, M., Kvas, A., Klinger, B., Strasser, S., and Zehentner, N.: ITSG-Grace2018 - Monthly, Daily and Static Gravity Field Solutions from GRACE, GFZ DataServices, 10.5880/ICGEM.2018.003, 2018.
Moreira, D. M., Calmant, S., Perosanz, F., Xavier, L., Rotunno Filho, O. C., Seyler, F., and Monteiro, A. C.: Comparisons of observed and modeled elastic responses to hydrological loading in the Amazon basin, Geophysical Research Letters, 43, 9604-9610, 10.1002/2016gl070265, 2016.
Ni, S., Chen, J., Wilson, C. R., Li, J., Hu, X., and Fu, R.: Global Terrestrial Water Storage Changes and Connections to ENSO Events, Surv Geophys, 39, 1-22, 10.1007/s10712-017-9421-7, 2017.
Oki, T., Musiake, K., Matsuyama, H., and Masuda, K.: Global atmospheric water balance and runoff from large river basins, Hydrological Processes, 9, 655-678, 10.1002/hyp.3360090513, 1995.
Pan, Y., Zhang, C., Gong, H., Yeh, P. J. F., Shen, Y., Guo, Y., Huang, Z., and Li, X.: Detection of human-induced evapotranspiration using GRACE satellite observations in the Haihe River basin of China, Geophysical Research Letters, 44, 190-199, 10.1002/2016gl071287, 2017.
Peltier, W. R., Argus, D. F., and Drummond, R.: Space geodesy constrains ice age terminal deglaciation: The global ICE-6G_C (VM5a) model, Journal of Geophysical Research-Solid Earth, 120, 450-487, 2015.

Reager, J. T., Gardner, A. S., Famiglietti, J. S., Wiese, D. N., Eicker, A., and Lo, M. H.: A decade of sea level rise slowed by climate-driven hydrology, Science, 351, 699-703, 2016.
Rietbroek, R., Brunnabend, S.-E., Kusche, J., Schröter, J., and Dahle, C.: Revisiting the contemporary sea-level budget on global and regional scales, Proceedings of the National Academy of Sciences, 113, 1504-1509, 10.1073/pnas.1519132113, 2016.
Rodell, M., Velicogna, I., and Famiglietti, J. S.: Satellite-based estimates of groundwater depletion in India, Nature, 460, 999-1002, 2009.
Rodell, M., Famiglietti, J. S., Wiese, D. N., Reager, J. T., Beaudoing, H. K., Landerer, F. W., and Lo, M. H.: Emerging trends in global freshwater availability, Nature, 557, 651-659, 10.1038/s41586-018-0123-1, 2018.
Roemmich, D., and Gilson, J.: The 2004–2008 mean and annual cycle of temperature, salinity, and steric height in the global ocean from the Argo Program, Progress in Oceanography, 82, 81-100, 10.1016/j.pocean.2009.03.004, 2009.
Rudd, A. C., Bell, V. A., and Kay, A. L.: National-scale analysis of simulated hydrological droughts (1891–2015), Journal of Hydrology, 550, 368-385, 10.1016/j.jhydrol.2017.05.018, 2017.
Scanlon, B. R., Zhang, Z., Save, H., Sun, A. Y., Müller Schmied, H., van Beek, L. P. H., Wiese, D. N., Wada, Y., Long, D., Reedy, R. C., Longuevergne, L., Döll, P., and Bierkens, M. F. P.: Global models underestimate large decadal declining and rising water storage trends relative to GRACE satellite data, Proceedings of the National Academy of Sciences, 115, E1080-E1089, 10.1073/pnas.1704665115, 2018.
Schellekens, J., Dutra, E., Martínez-de la Torre, A., Balsamo, G., van Dijk, A., Sperna Weiland, F., Minvielle, M., Calvet, J.-C., Decharme, B., Eisner, S., Fink, G., Flörke, M., Peßenteiner, S., van Beek, R., Polcher, J., Beck, H., Orth, R., Calton, B., Burke, S., Dorigo, W., and Weedon, G. P.: A global water resources ensemble of hydrological models: the eartH2Observe Tier-1 dataset, Earth Syst Sci Data, 9, 389-413, 10.5194/essd-9-389-2017, 2017.
Seneviratne, S. I., Viterbo, P., Lüthi, D., and Schär, C.: Inferring Changes in Terrestrial Water Storage Using ERA-40 Reanalysis Data: The Mississippi River Basin, Journal of Climate, 17, 2039-2057, 10.1175/1520-0442(2004)017<2039:icitws>2.0.co;2, 2004.
Sheffield, J., and Wood, E. F.: Projected changes in drought occurrence under future global warming from multi-model, multi-scenario, IPCC AR4 simulations, Climate Dynamics, 31, 79-105, 10.1007/s00382-007-0340-z, 2007.
Sheffield, J., Wood, E. F., and Roderick, M. L.: Little change in global drought over the past 60 years, Nature, 491, 435-+, 2012.
Sinha, D., Syed, T. H., Famiglietti, J. S., Reager, J. T., and Thomas, R. C.: Characterizing Drought in India Using GRACE Observations of Terrestrial Water Storage Deficit, Journal of Hydrometeorology, 18, 381-396, 10.1175/jhm-d-16-0047.1, 2017.
Spinoni, J., Naumann, G., and Vogt, J. V.: Pan-European seasonal trends and recent changes of drought frequency and severity, Global and Planetary Change, 148, 113-130, 10.1016/j.gloplacha.2016.11.013, 2017.
Sutanudjaja, E. H., van Beek, L. P. H., de Jong, S. M., van Geer, F. C., and Bierkens, M. F. P.: Large-scale groundwater modeling using global datasets: a test case for the Rhine-Meuse basin, Hydrology and Earth System Sciences, 15, 2913-2935, 10.5194/hess-15-2913-2011, 2011.
Sutanudjaja, E. H., van Beek, L. P. H., de Jong, S. M., van Geer, F. C., and Bierkens, M. F. P.: Calibrating a large-extent high-resolution coupled groundwater-land surface model using soil moisture and discharge data, Water Resources Research, 50, 687-705, 10.1002/2013wr013807, 2014.
Um, M.-J., Kim, Y., and Kim, J.: Evaluating historical drought characteristics simulated in CORDEX East Asia against observations, International Journal of Climatology, 37, 4643-4655, 10.1002/joc.5112, 2017.
van Beek, L. P. H., and Bierkens, M. F. P.: The Global Hydrological Model PCR-GLOBWB: Conceptualization, Parameterization and Verification, Available at: http:/vanbeek.geo.uu.nl/suppinfo/vanbeekbierkens2009.pdf, 2008.
van Beek, L. P. H., Wada, Y., and Bierkens, M. F. P.: Global monthly water stress: 1. Water balance and water availability, Water Resources Research, 47, 10.1029/2010wr009791, 2011.
Van Der Knijff, J. M., Younis, J., and De Roo, A. P. J.: LISFLOOD: a GIS-based distributed model for river basin scale water balance and flood simulation, Int J Geogr Inf Sci, 24, 189-212, 2010.
van Dijk, A. I. J. M., Peña-Arancibia, J. L., Wood, E. F., Sheffield, J., and Beck, H. E.: Global analysis of seasonal streamflow predictability using an ensemble prediction system and observations from 6192 small catchments worldwide, Water Resources Research, 49, 2729-2746, 10.1002/wrcr.20251, 2013.
van Dijk, A. I. J. M., Renzullo, L. J., Wada, Y., and Tregoning, P.: A global water cycle reanalysis (2003–2012) merging satellite gravimetry and altimetry observations with a hydrological multi-model ensemble, Hydrology and Earth System Sciences, 18, 2955-2973, 10.5194/hess-18-2955-2014, 2014.
Veldkamp, T. I. E., Eisner, S., Wada, Y., Aerts, J. C. J. H., and Ward, P. J.: Sensitivity of water scarcity events to ENSO-driven climate variability at the global scale, Hydrology and Earth System Sciences, 19, 4081-4098, 10.5194/hess-19-4081-2015, 2015.
Vergnes, J. P., Decharme, B., and Habets, F.: Introduction of groundwater capillary rises using subgrid spatial variability of topography into the ISBA land surface model, J Geophys Res-Atmos, 119, 11065-11086, 2014.
Wada, Y., van Beek, L. P. H., Viviroli, D., Dürr, H. H., Weingartner, R., and Bierkens, M. F. P.: Global monthly water stress: 2. Water demand and severity of water stress, Water Resources Research, 47, 10.1029/2010wr009792, 2011.
Wada, Y., Wisser, D., and Bierkens, M. F. P.: Global modeling of withdrawal, allocation and consumptive use of surface water and groundwater resources, Earth System Dynamics, 5, 15-40, 10.5194/esd-5-15-2014, 2014.

Wada, Y., Reager, J. T., Chao, B. F., Wang, J., Lo, M.-H., Song, C., Li, Y., and Gardner, A. S.: Recent Changes in Land Water Storage and its Contribution to Sea Level Variations, Surv Geophys, 38, 131-152, 10.1007/s10712-016-9399-6, 2016.
Wahr, J.: Time-Variable Gravity from Satellites, in: Treatise on Geophysics, Second Edition ed., edited by: Schubert, G., Elsevier, Oxford, 193-213, 2015.
Watkins, M. M., Wiese, D. N., Yuan, D. N., Boening, C., and Landerer, F. W.: Improved methods for observing Earth's time variable mass distribution with GRACE using spherical cap mascons, J Geophys Res-Sol Ea, 120, 2648-2671, 10.1002/2014JB011547, 2015.
Wiese, D. N., Landerer, F. W., and Watkins, M. M.: Quantifying and reducing leakage errors in the JPL RL05M GRACE mascon solution, Water Resources Research, 52, 7490-7502, 10.1002/2016WR019344, 2016.
Wilks, D. S.: Statistical methods in the atmospheric sciences, 3rd Edition ed., International Geophysics Series, 2011.
Wouters, B., Bonin, J. A., Chambers, D. P., Riva, R. E. M., Sasgen, I., and Wahr, J.: GRACE, time-varying gravity, Earth system dynamics and climate change, Reports on Progress in Physics, 77, 116801, 2014.
Youm, K., Seo, K.-W., Jeon, T., Na, S.-H., Chen, J., and Wilson, C. R.: Ice and groundwater effects on long term polar motion (1979–2010), Journal of Geodynamics, 106, 66-73, 10.1016/j.jog.2017.01.008, 2017.
Zhang, L., Dobslaw, H., Stacke, T., Güntner, A., Dill, R., and Thomas, M.: Validation of terrestrial water storage variations as simulated by different global numerical models with GRACE satellite observations, Hydrology and Earth System Sciences, 21, 821-837, 10.5194/hess-21-821-2017, 2017.

Table 1. GRACE datasets used for model calibration

GRACE product	Time period	Spatial resolution	GIA correction	Access	Citation
JPL-Mascons RL06 with CRI	April 2002 - June 2017	3° equal-area mascons, sampled on a 0.5° grid	(A et al., 2013)	ftp://podaac-ftp.jpl.nasa.gov/allData/tellus/L3/mascon/RL06/JPL/CRI/netcdf/	(Watkins et al., 2015;Wiese et al., 2016)
GSFC-Mascons v2.4, ICE6G	January 2003 - July 2016	1° equal-area mascons, sampled on a 0.5° grid	(Peltier et al., 2015)	https://neptune.gsfc.nasa.gov/gngphys/index.php?section=456products.html	(Luthcke et al., 2013)

Supprimé: 5

Supprimé: ftp://podaac.jpl.nasa.gov/allData/tellus/L3/mascon/RL05/JPL/CRI/

Table 2. Meteorological forcing datasets

Dataset	Time period	Spatial resolution used	Description	Access	Citation
MSWEP v2.2	1979-2016	0.5° grid	Merged precipitation product combining multiple data sources	http://www.gloh2o.org/	(Beck et al., 2018)
ERA5	1979-current	0.5° grid	Atmospheric reanalysis with regular updates	https://cds.climate.copernicus.eu/#!/search?text=ERA5&type=dataset	(Hersbach and Dee, 2016)
GSWP3 v1.1	1901-2014	0.5° grid	ERA 20th Century Reanalysis, downscaled to 0.5° resolution using spectral nudging and bias-corrected with GPCP and CRU	http://www.dias.nii.ac.jp/gswp3/input.html	(Kim, 2017)

Supprimé: -Interim

Supprimé: http://apps.ecmwf.int/datasets/data/interim-full-daily/levtype=sfc/

Table 3. List of the 6 GRACE-REC datasets available at monthly and daily scale

GRACE-REC dataset	Time period	Spatial resolution	Forcing data	Training data	Unit
JPL-MSWEP	1979-2016	3° equal-area (provided on a 0.5° grid)	MSWEP & ERA5	GRACE JPL	mm TWS
JPL-GSWP3	1901-2014		GSWP3		
JPL-ERA5	1979-current		ERA5		
GSFC-MSWEP	1979-2016	1° equal-area (provided on a 0.5° grid)	MSWEP & ERA5	GRACE GSFC	
GSFC-GSWP3	1901-2014		GSWP3		
GSFC-ERA5	1979-current		ERA5		

Supprimé: I

Supprimé: -Interim

Supprimé: I

Supprimé: -Interim

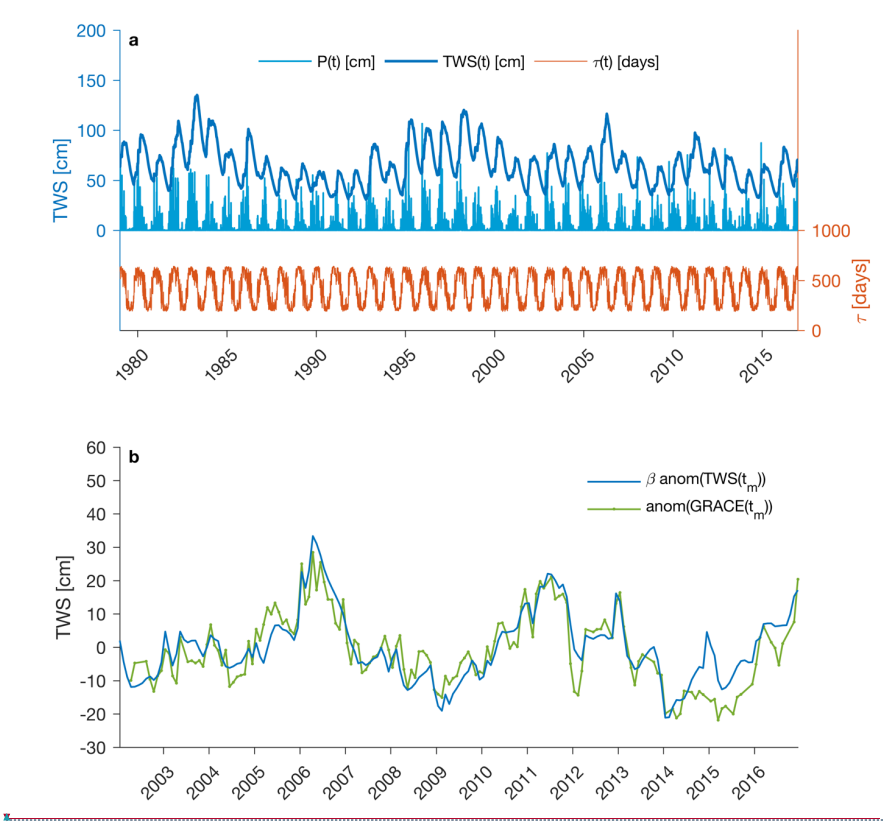

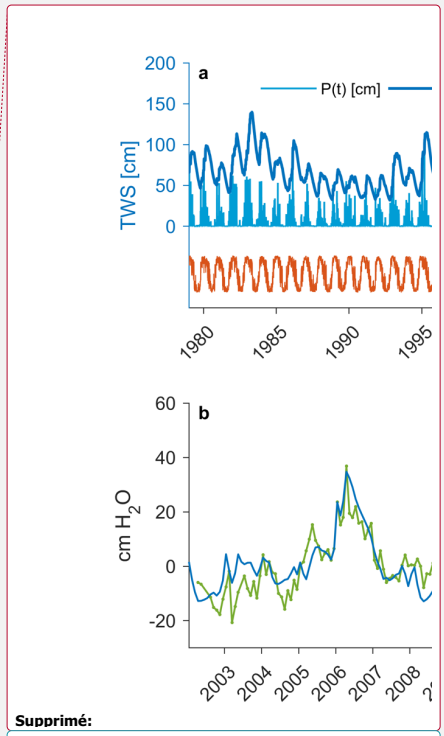

Supprimé:

Mis en forme: Police :(par défaut) Helvetica

Figure 1. Illustration of the GRACE reconstruction at one given 3° x 3° mascon (located in California). (a) Input daily precipitation time series $P(t)$, temperature-dependent residence time $\tau(t)$, and the resulting daily TWS time series $TWS(t)$. (b) Agreement between GRACE and GRACE-REC after subtracting the seasonal cycle and long-term trend (zoomed over the period 2002-2017).

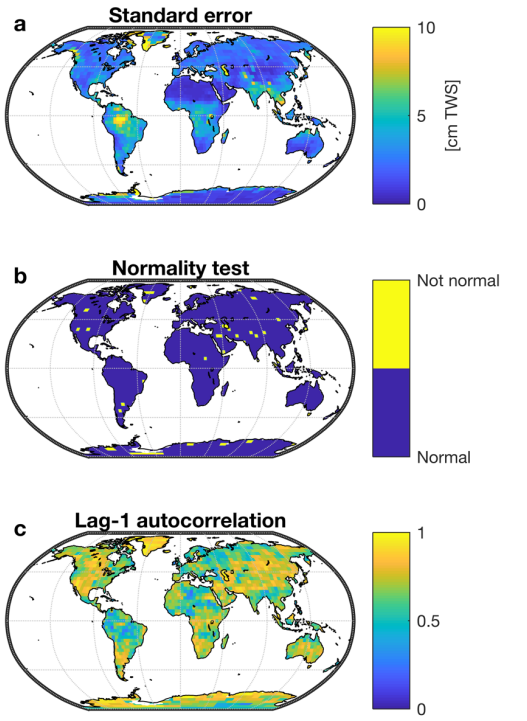

Figure 2. Characterization of the empirical model residuals for the GRACE-REC dataset based on MSWEP precipitation and ERA5 air temperature, calibrated with the JPL mascons. (a) Standard model error, (b) Result of a Kolmogorov-Smirnov test for normality on the model errors ($p<0.05$), (c) lag-1 serial autocorrelation of the model errors.

Supprimé:

Supprimé: -Interim

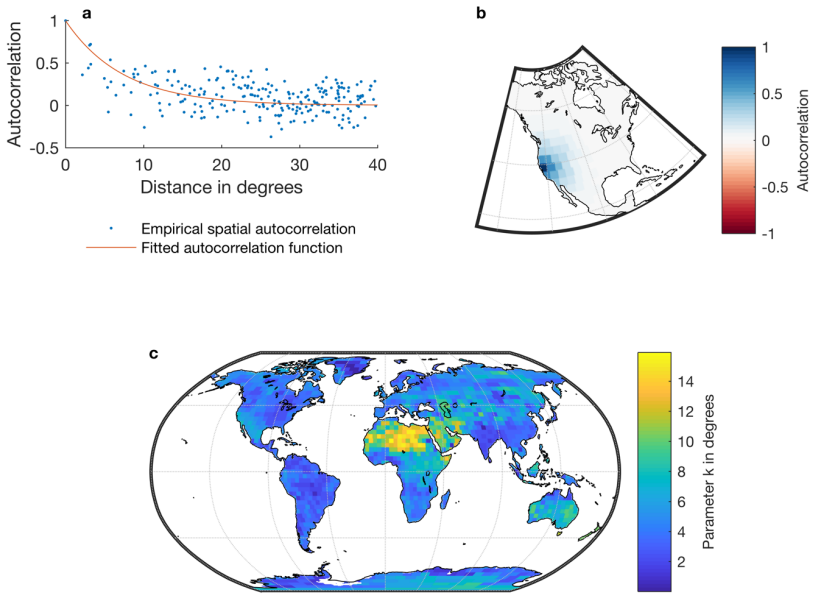

Supprimé:

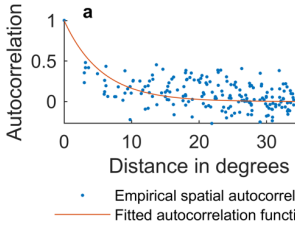

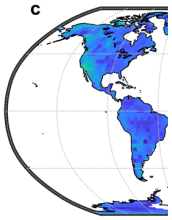

Figure 3. Illustration of the spatial autocorrelation of the empirical model residuals and their representation in the SAR model (for the GRACE-REC product based on MSWEP and calibrated with JPL Mascons). (a) Empirical and fitted spatial autocorrelation functions for the model residuals at a given 3° x 3° mascon in California. (b) Fitted spatial autocorrelation at that mascon. (c) Fitted parameter k (Eq. 11), which conditions the steepness of the autocorrelation function (high values = high autocorrelation length of the residuals).

Supprimé: also

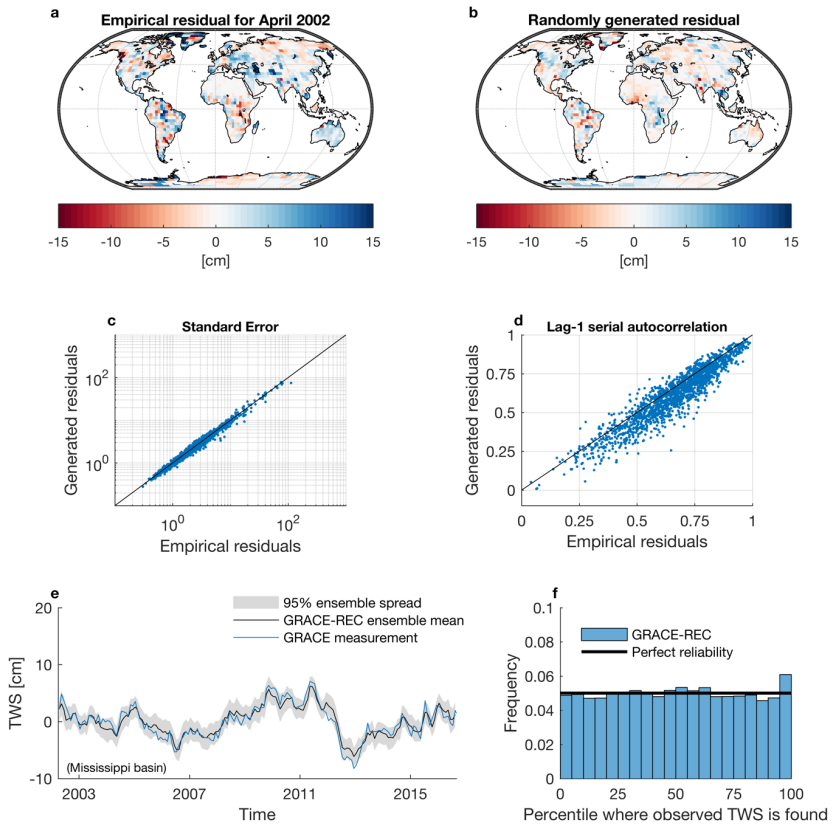

Supprimé:

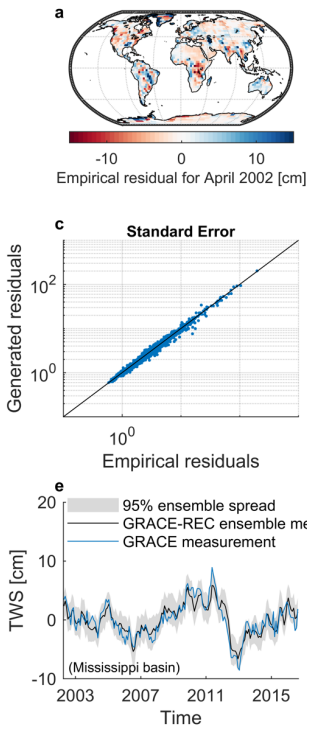

Figure 4. Output of the SAR model for the generation of random noise realisations that have a spatio-temporal structure similar to that of the empirical model residuals (for the GRACE-REC product based on MSWEP and calibrated with JPL Mascons). (a) Empirical model residual at a given time step. (b) Residual randomly generated by the SAR model. (c) Agreement between the standard deviation of the empirical versus generated residuals (each point represents one mascon). (d) Agreement between the lag-1 autocorrelation of the empirical versus generated residuals (each point represents one mascon). (e)

Illustration of the resulting ensemble spread for a basin-scale average. (f) Rank histogram using 5% bins, combining the data for 90 large (>500'000 km^2) basins (from 2003 to 2014), used to evaluate the reliability of ensemble forecasts.

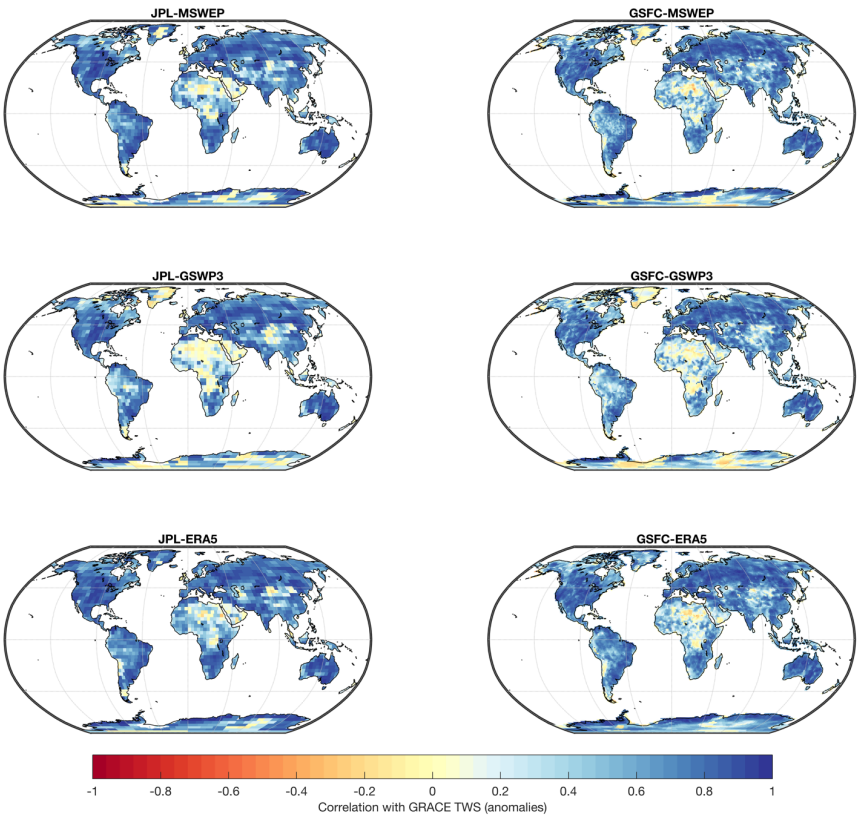

Figure 5. Correlation (of de-seasonalized, de-trended anomalies) between GRACE-REC and GRACE JPL Mascons (left column), or GRACE GSFC Mascons (right column). Three different precipitation forcing datasets are tested: MSWEP (top row), GSWP3 (middle row), and ERA5 (bottom row). Values closer to one correspond to a higher model performance.

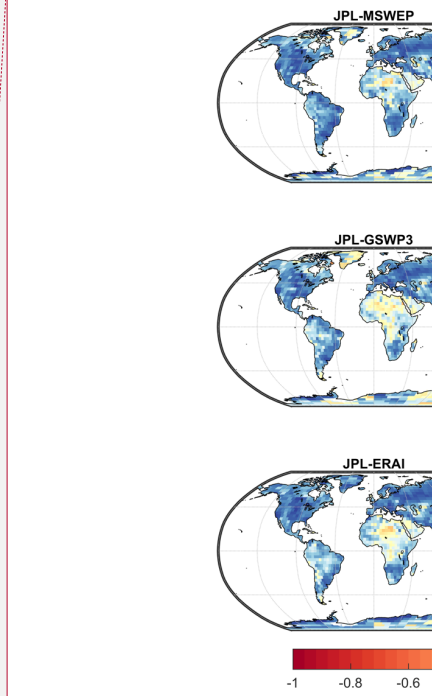

Supprimé:

Mis en forme: Justifié, Interligne : 1,5 ligne

Supprimé: -Interim

Supprimé: .

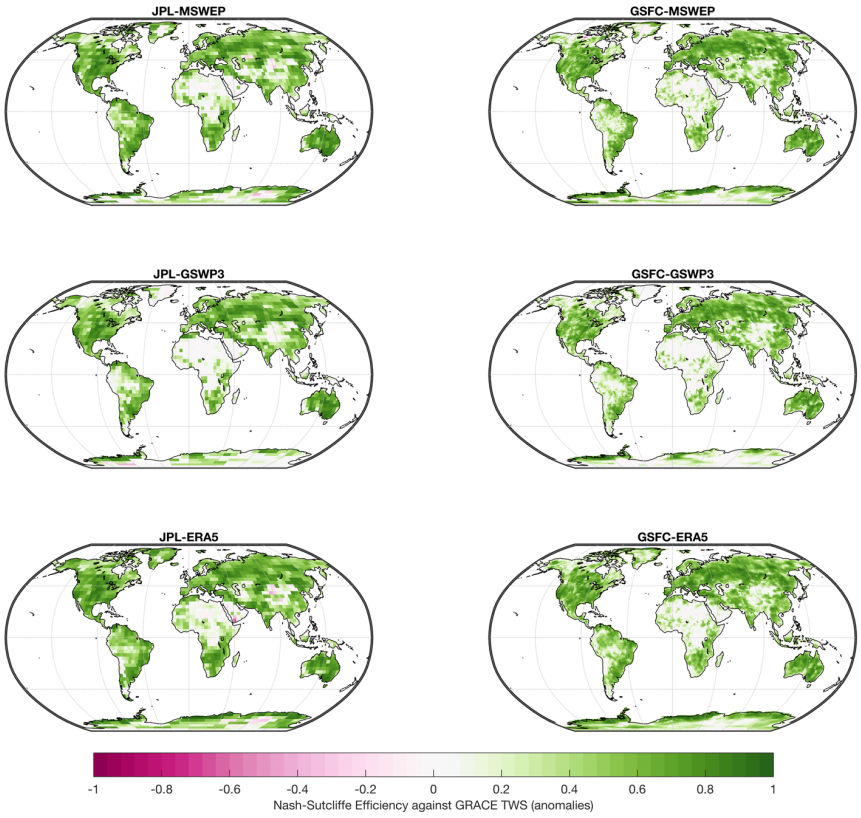

Figure 6. Nash-Sutcliffe Efficiency (of de-seasonalized, de-trended anomalies) between GRACE-REC and GRACE JPL Mascons (left column), or GRACE GSFC Mascons (right column). Three different precipitation forcing datasets are tested: MSWEP (top row), GSWP3 (middle row), and ERA5 (bottom row). Values closer to one correspond to a higher model performance.

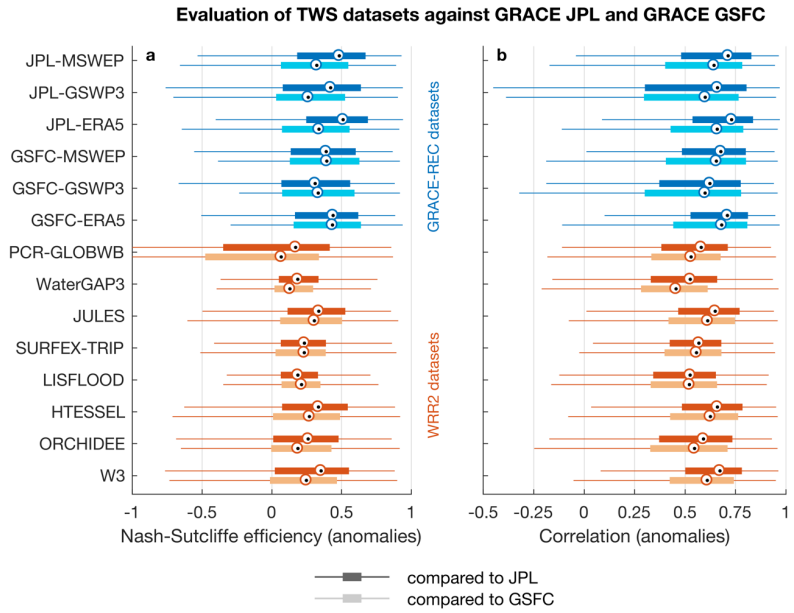

Figure 7. Global area-weighted box plots of the performance metrics shown in Figures 5 and 6 for GRACE-REC datasets (blue), and comparison with the performance of global hydrological models participating in the Earth2Observe Water Resources Reanalysis version 2 (WRR2) (orange). Dark colors indicate the performance obtained when comparing against 3° x 3° JPL Mascons, and against 1° x 1° GSFC Mascons for light colors. Note: WRR2 models are driven with MSWEP precipitation and all model outputs are aggregated to the resolution of the corresponding GRACE dataset. Greenland and Antarctica are always excluded.

Supprimé: Evaluation of TWS d

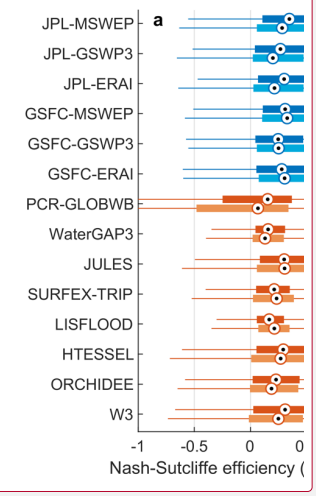

Supprimé:

Supprimé: Global summary

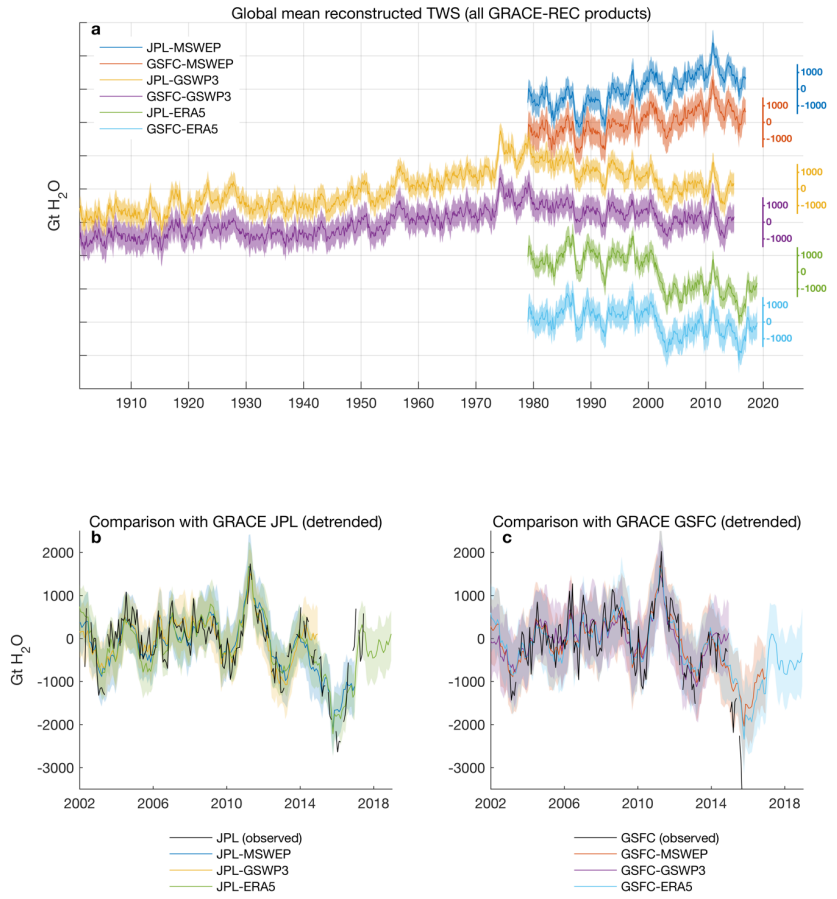

Figure 8. (a) Global average of TWS anomalies for the 6 GRACE-REC datasets (excluding Greenland and Antarctica) with an artificial vertical offset added for better visual comparison. (b) Comparison of the 3 GRACE-REC datasets calibrated with GRACE JPL against GRACE JPL (de-trended anomalies). (c) Same as (b) but for GRACE GSFC.

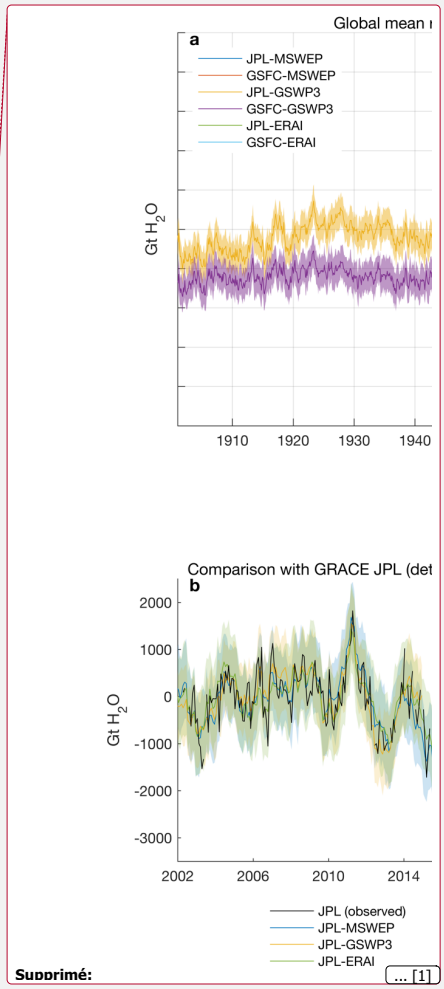

Supprimé: ... [1]

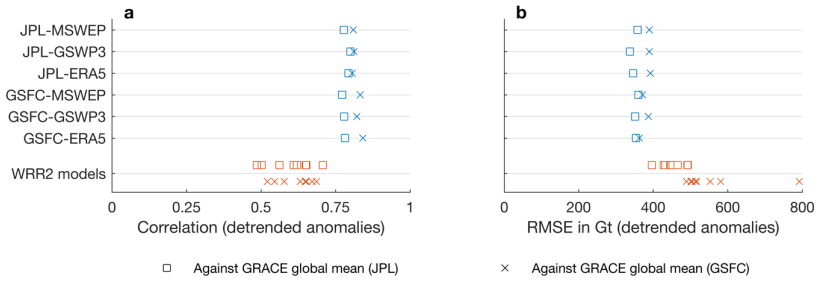

Figure 9. Agreement of the global average of different TWS model estimates (from GRACE-REC (blue) and WRR2 models (orange)) with the observed TWS anomalies from JPL (squares) and GSFC (crosses) solutions.

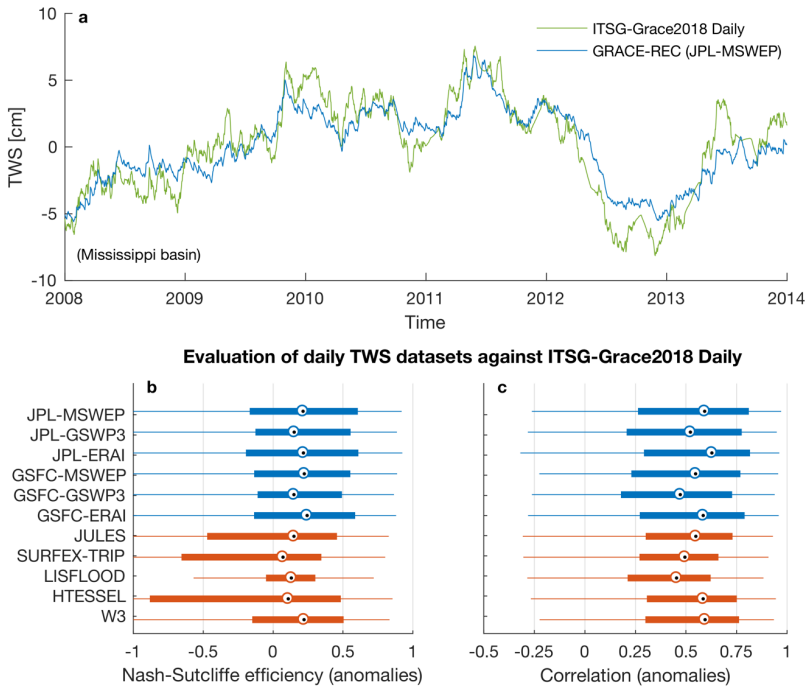

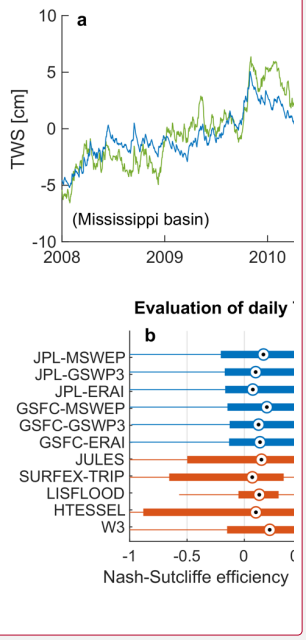

Supprimé:

Figure 10. (a) Comparison between the GRACE-REC daily TWS reconstruction (JPL-MSWEP dataset) and the daily GRACE JTSG-Grace2018 solution for the Mississippi basin (focused over the period 2008-2014 to improve readability of the high-frequency fluctuations). (b-c) Global area-weighted box plots of the performance metrics of the daily TWS datasets when compared with JTSG-Grace2018 at a spatial resolution of 5°. Note that some WRR2 models are not included because not all water storage variables were available to us at daily frequency. Greenland and Antarctica are excluded.

Supprimé: ITSG2018

Supprimé: Summary

Supprimé: ITSG2018

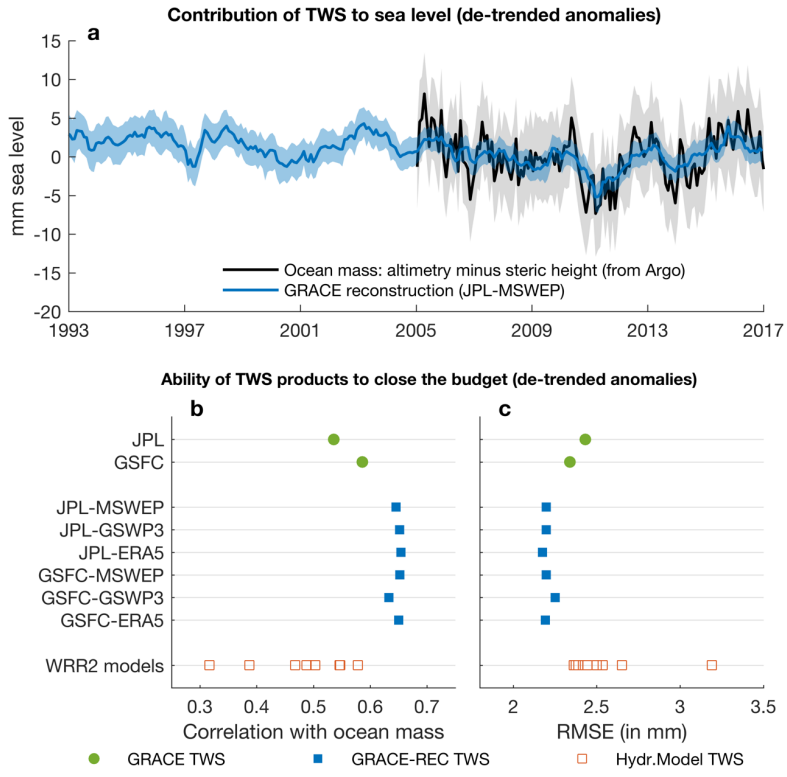

Figure 11. (a) Comparison of the global mean TWS reconstructed by GRACE-REC (converted to equivalent mm sea level) against the ocean mass derived from the sea level budget. (b-c) Evaluation of the ability of various TWS datasets to close the sea level budget (GRACE estimates in green, GRACE-REC datasets in blue, and WRR2 models in orange).

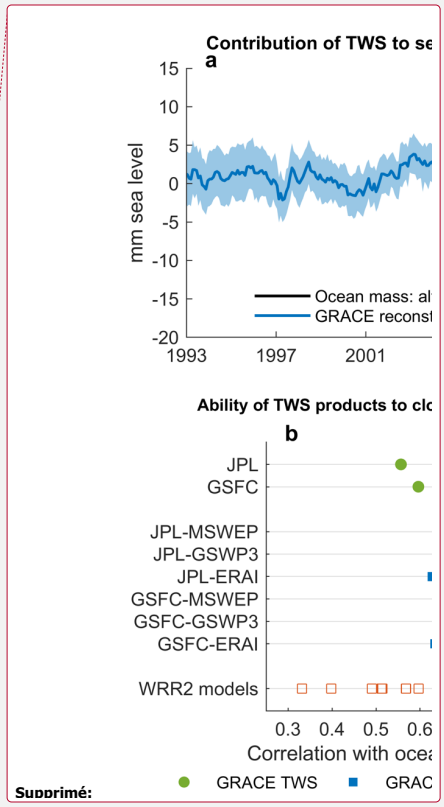

Supprimé:

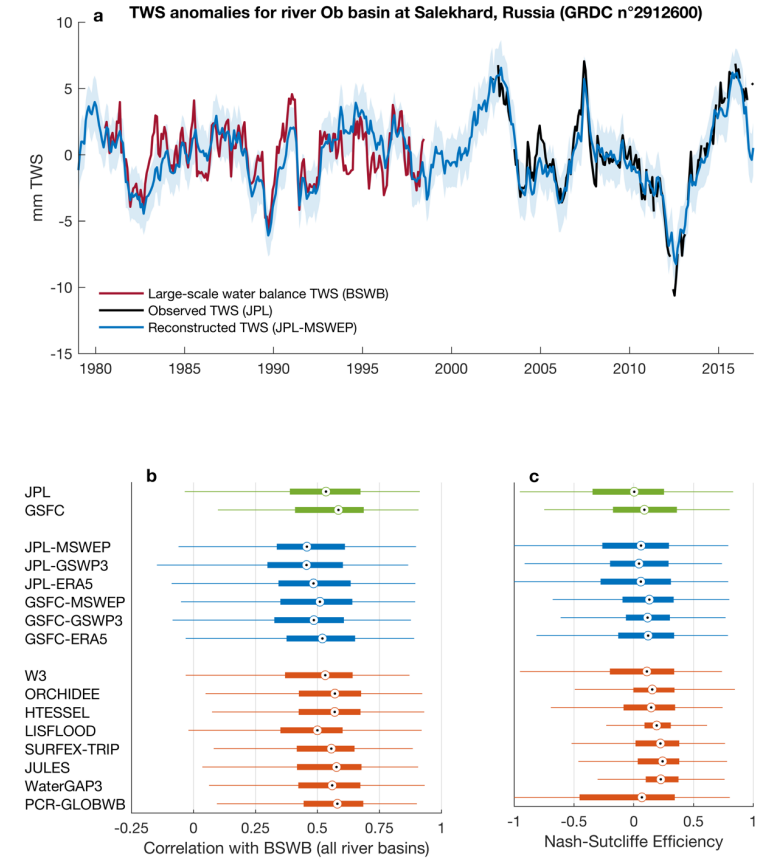

Figure 12. (a) Comparison between TWS anomalies derived from atmospheric basin-scale water balance (BSWB), GRACE observations (JPL) and the GRACE reconstruction (JPL-MSWEP dataset). (b-c) Global box plots of the agreement between various TWS products and BSWB estimates (based on the performance metrics at 341 large basins). The scale factors were applied to the JPL data for this specific analysis.

Supprimé: Overall evaluation

Supprimé: of

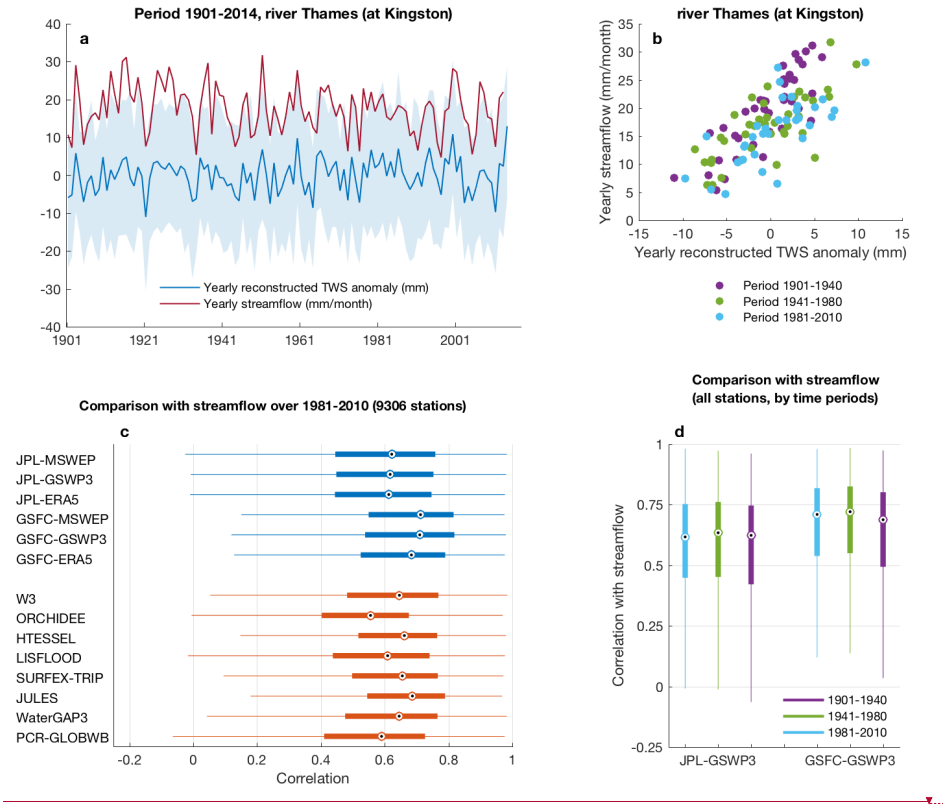

Figure 13. (a) Comparison between century-long measurements of streamflow and the TWS anomalies reconstructed at this location (GSFC-GSWP3 dataset). (b) Scatter plot of the data in (a), by time period. (c) Global box plots of the performance of GRACE-REC and WRR2 models when compared with yearly streamflow anomalies. (d) Global box plots of the performance of the JPL-GSWP3 and GSFC-GSWP3 products when compared with yearly streamflow anomalies, by time period (n=1274, 8065 and 9306 for 1901-40, 1941-80 and 1981-2010 respectively).

Supprimé: Evaluation

Supprimé: Evaluation

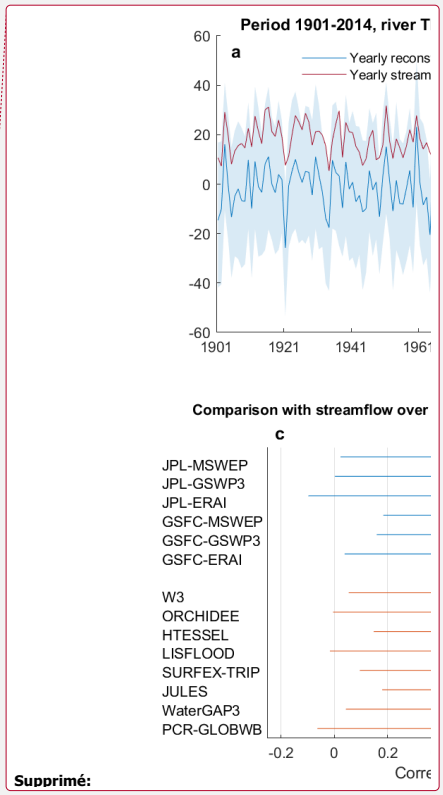

Supprimé: